Title

Abatacept/Ruxolitinib and Screening for Concomitant Respiratory Muscle Failure to Mitigate Fatality of Immune-Checkpoint Inhibitor Myocarditis.

Journal

Cancer Discovery, 13(5)

ISSN

2159-8274

Authors

Salem, Joe-Elie
Bretagne, Marie
Abbar, Baptiste
et al.

Publication Date

2023-05-04

DOI

10.1158/2159-8290.cd-22-1180

Peer reviewed

Immune-Checkpoint Inhibitor Myocarditis – Abatacept/Ruxolitinib and screening for concomitant respiratory muscle failure to mitigate fatality

Short title: Management of immune checkpoint inhibitor myotoxicity

Joe-Elie SALEM, MD, PhD[1]; Marie BRETAGNE, MD[1]; Baptiste ABBAR, MD[1,2] ; Sarah LEONARD-LOUIS, MD[3]; Stéphane EDERHY, MD[4]; Alban REDHEUIL, MD, PhD[5]; Samia BOUSSOUAR, MD[5]; Lee S NGUYEN, MD[1,6], Adrien PROCUREUR, MD[1]; Frederic STEIN, MD[1]; Charlotte FENIOUX, MD[1]; Perrine DEVOS, MD[1]; Paul GOUGIS, MD[1]; Martin DRES, MD, PhD[7]; Alexandre DEMOULE, MD, PhD[7]; Dimitri PSIMARAS, MD[8]; Timothee LENGLET, MD[8]; Thierry MAISONOBE, MD[8]; Marc PINETON DE CHAMBRUN, MD, PhD[9]; Guillaume HEKIMIAN MD[9]; Christian STRAUS, MD, PhD[10]; Jesus GONZALEZ-BERMEJO, MD, PhD[7]; David KLATZMANN, MD, PhD[11]; Aude RIGOLET, MD[12], Perrine GUILLAUME-JUGNOT, MD[12]; Nicolas CHAMPTIAUX, MD[12]; Olivier BENVENISTE, MD, PhD[12]; Nicolas WEISS, MD, PhD[13]; Samir SAHEB, MD[14]; Philippe ROUVIER, MD[15]; Isabelle PLU, MD, PhD[3]; Estelle GANDJBAKHCH, MD, PhD[16]; Mathieu KERNEIS, MD, PhD[16]; Nadjib HAMMOUDI, MD, PhD[16]; Noel ZAHR, MD, PhD[1]; Claudia LLONTOP, MD[7]; Capucine MORELOT-PANZINI, MD, PhD[7]; Lorenz LEHMANN, MD[17]; Juan QIN, PhD[18]; Javid MOSLEHI, MD[18]; Michelle ROSENZWAJG, MD, PhD[11]; Thomas SIMILOWSKI, MD, PhD[7]; Yves ALLENBACH, MD, PhD[12]

[1] Sorbonne Université, INSERM, UNICO-GRECO Cardio-oncology Program, Department of Pharmacology, GRC27, CIC-1901, AP-HP, Hôpital Pitié-Salpêtrière, F-75013 Paris, France
[2] Sorbonne Université, INSERM, Department of Oncology, AP-HP, Hôpital Pitié-Salpêtrière, F-75013 Paris, France
[3] Sorbonne Université, INSERM, Department of Neuropathology, AP-HP, Hôpital Pitié-Salpêtrière, F-75013 Paris, France
[4] Sorbonne Université, INSERM, UNICO-GRECO Cardio-oncology Program, Department of Cardiology, GRC27, AP-HP, Hôpital Saint-Antoine, F-75012 Paris, France
[5] Sorbonne Université, INSERM, ICAN, Department of Radiology, AP-HP, Hôpital Pitié-Salpêtrière, F-75013 Paris, France
[6] Research and Innovation of CMC Ambroise Paré (RICAP), Centre Medico-Chirurgical Ambroise Paré, Neuilly-sur-Seine, France
[7] Sorbonne Université, INSERM, Department R3S (Respiration, Réanimation, Réhabilitation, Sommeil), AP-HP, Hôpital Pitié-Salpêtrière, F-75013 Paris, France
[8] Sorbonne Université, INSERM, Department of Neurology, AP-HP, Hôpital Pitié-Salpêtrière, F-75013 Paris, France
[9] Sorbonne Université, INSERM, ICAN, Department of Medical Intensive Care Unit, AP-HP, Hôpital Pitié-Salpêtrière, F-75013 Paris, France
[10] Sorbonne Université, INSERM, UMRS1158, Service d'Explorations Fonctionnelles de la Respiration, de l'Exercice et de la Dyspnée (Département R3S), AP-HP, Hôpital Pitié-Salpêtrière, F-75013 Paris, France
[11] Sorbonne University, INSERM UMRS959, Assistance Publique Hôpitaux de Paris, Hôpital Pitié-Salpêtrière, CIC-1901, Paris, France
[12] Sorbonne Université, INSERM, Department of Internal Medicine, AP-HP, Hôpital Pitié-Salpêtrière, F-75013 Paris, France
[13] Sorbonne Université, INSERM, Department of Neurology intensive care unit, AP-HP, Hôpital Pitié-Salpêtrière, F-75013 Paris, France
[14] Sorbonne Université, INSERM, Department of Hemobiology, AP-HP, Hôpital Pitié-Salpêtrière, F-75013 Paris, France
[15] Sorbonne Université, INSERM, Department of Anatomopathology, AP-HP, Hôpital Pitié-Salpêtrière, F-75013 Paris, France
[16] Sorbonne Université, ACTION Study Group, INSERM UMR_S 1166, Institute of Cardiometabolism And Nutrition (ICAN), and Hôpital Pitié-Salpêtrière (AP-HP), Boulevard de l'hôpital, F-75013, Paris, France.
[17] Department of Cardiology, Angiology, and Pneumology, Heidelberg University Hospital, Heidelberg, Germany; German Centre for Cardiovascular Research (DZHK), Heidelberg/Mannheim partner site, Germany
[18] Section of Cardio-Oncology & Immunology, Division of Cardiology and the Cardiovascular Research Institute, University of California San Francisco, 555 Mission Bay Blvd South, Box 3118, San Francisco, CA 94143-3118

Correspondence: joe-elie.salem@aphp.fr, CIC-1901, Departement of Clinical Pharmacology, Pitié-Salpêtrière University Hospital, Sorbonne Universite; 47 Boulevard de l'Hopital, 75013 PARIS ;

Abstract/Manuscript word counts: **150/150; 4244**
Figures: 8
Tables: 2
References: 48

Conflict of interest/Disclosures. JES has participated to advisory boards or consultancy from BMS, Novartis, Banook, AstraZeneca and Beigene. BA has participated to advisory boards or consultancy from Novartis, Sanofi and Astellas. SE received modest consultant fees from AstraZeneca, Amgen, BMS, Banook, Celgene, Siemens and Eisai. GH received lecture fees from Stago Biocare. AD reports grants from Lungpacer, Respinor, consulting fees from Respinor, Lungpace, Lowenstein, or honoraria for lectures from Fisher & Paykel, Baxter, Getinge, Astra, Agence Européenne Informatique, Mindray, and support for attending meetings and/or travel from Lungpacer, outside the submitted work. NH reports consulting/lecture fees from Abbott Medical, Bayer, Boehringer Ingelheim, Novartis, Philips. MK received fees from Bayer, Sanofi, Kiniksa, and Eligo. EG reports consulting fees from abbott, microport, Medtronic, outside the submitted work. JJM has served on advisory boards for Bristol Myers Squibb, Takeda, Audentes, Deciphera, Janssen, Amgen, Myovant, Kurome Therapeutics, Star Therapeutics, Pharmacyclics, Pfizer, Mallinckrodt Pharmaceuticals, Silverback Therapeutics, TranshteraBio, Prelude Therapeutics, Kiniksa, Beigine, Cytokinetics, and AstraZeneca. JJM was supported by National Institutes of Health grants (R01HL141466, R01HL155990, and R01HL156021). TS reports consultancy fees from Lungpacer, ADEP assistance, AstraZeneca, Chiesi, KPL, Novartis, TEVA, Vitalaire. JES, JJM, MK and YA have patents related to the treatment of ICI related immune adverse events. Other authors have nothing to disclose regarding this manuscript.

Funding. This study was funded by CIC-1901.

Acknowledgment. We would really like to thank Pr. Dan M RODEN (Vanderbilt University Medical Center, Nashville, TN) for his critical support in editing this work.

Abstract.

Immune-checkpoint-inhibitor (ICI)-associated myotoxicity involves the heart (myocarditis) and skeletal muscles (myositis), which frequently occur concurrently and is highly fatal. We report the results of a strategy that included identification of individuals with severe ICI-myocarditis by also screening for and managing concomitant respiratory muscle involvement with mechanical ventilation, as well as treatment with CTLA4-fusion protein abatacept and the Janus-kinase inhibitor ruxolitinib. Forty cases with definite ICI-myocarditis were included with pathological confirmation of concomitant myositis in the majority of patients. In the first 10 patients, using recommended guidelines, myotoxicity-related fatality occurred in 60%, consistent with historical controls. In the subsequent 30 cases, we instituted systematic screening for respiratory muscle involvement coupled with active ventilation and treatment using ruxolitinib and abatacept. Abatacept dose was adjusted using CD86-receptor occupancy on circulating monocytes. Myotoxicity-related fatality rate was 3.4%(1/30) in these 30 patients vs.60% in 1st quartile($p<0.0001$). These clinical results are hypothesis-generating and need further evaluation.

Statement of significance.

Early management of respiratory muscle failure using mechanical ventilation and high-dose abatacept with CD86 receptor occupancy monitoring combined with ruxolitinib may be promising to mitigate high fatality rates in severe Immune-Checkpoint Inhibitor myocarditis.

Introduction.

Immune-checkpoint inhibitors (ICI) have revolutionized cancer treatment and have been approved in multiple cancer types, and include antibodies that target CTLA4 (cytotoxic-T-lymphocyte-antigen-4), PD1 (Programmed-cell-Death-protein 1), the PD1 ligand PDL1, and LAG3 (lymphocyte-activating-3).(1) ICI restore T-cell-mediated host immunity against tumors,(1) but they may also induce immune related adverse events (irAE)(2) including ICI-myocarditis which occurs infrequently (~1%) but carries a 30-50% mortality rate.(3-7) Clinical suspicion for ICI-myocarditis often arises after associated symptoms and increases in cardiac biomarkers (troponins) or electrocardiographic alterations.(3,8-10) Endomyocardial biopsy is the gold-standard for establishing the diagnosis,(10,11) while cardiac magnetic resonance imaging (cMRI) and echocardiography may be misleadingly normal especially early in the clinical course.(10,12,13) Other forms of myotoxicity often accompany myocarditis and these include peripheral myositis, which can affect respiratory muscles or mimic myasthenia-gravis-like syndrome.(6,10,14) The pathophysiology of these myotoxicities is characterized by myocyte necrosis induced by lympho-histiocytic infiltrates secondary to activation of clonal autoreactive T-cells against muscle antigens, notably α-myosin expressed in the heart and peripheral muscles.(7,15). Preliminary data suggest that myositis, particularly when affecting respiratory muscles, accompanying ICI-myocarditis can negatively impact survival, and requires an aggressive patient care strategy.(5,6,10,14) The main causes of death attributed to ICI-myotoxicities are life-threatening ventricular arrhythmias, cardiogenic shock or hypercapnic respiratory muscle failure.(10)

Current treatment of ICI-myocarditis includes empiric corticosteroids, which are not universally effective; second line therapies, including immunosuppressive therapies targeting T-cells have been described.(16-18) In pre-clinical models, CTLA4 signaling appears to play a critical role in the development of myocarditis with CTLA4 immunoglobulin(Ig)-fusion-protein (abatacept) attenuating myocardial inflammation.(19) Preliminary case reports have suggested that the CTLA4 immunoglobulin-fusion-protein abatacept may be a promising option.(19-21) However, the optimal dosing scheme and the effect of combining CTLA4-Ig with other immunosuppressants is unknown. Abatacept (a CTLA4-Ig), acts as a decoy receptor for CD80/CD86 expressed

on antigen-presenting-cells (e.g., macrophages), interfering with T-cell co-stimulation through CD28. Therefore, abatacept leads to global T-cell anergy by reversing pathways activated by ICI.(1,19-21) When abatacept is used for approved indications such as rheumatoid arthritis, occupancy of the CD86 receptor on circulating monocytes (CD86RO) is a pharmacodynamic biomarker of clinical activity, with CD86RO≥80% as a target for maximal efficacy.(22,23) Another consideration is time of onset of abatacept which is slow-onset. Consistently, in a mouse model of ICI-myocarditis, myocardial immune infiltration is attenuated after 10 weeks of abatacept treatment; 2-week duration of treatment with abatacept had minimal effect on immune infiltration.(19) Preliminary reports suggest that abatacept clinical efficacy can be enhanced by addition of the Janus kinase (JAK) inhibitor ruxolitinib, which impairs T-cell activation via blockade of pro-inflammatory cytokines and is used to treat graft vs. host disease, a condition in which donor T-cells attack host tissue.(21,24) Ruxolitinib (a JAK1, JAK2 inhibitor) is thought to exert a rapid (within hours of start) synergistic effect with abatacept (slower time to onset of effect) by also decreasing CD86 expression on macrophages while also acting downstream in the immunological synapse, inactivating T-cells.(1,25-27)

With these considerations in mind, we have developed a strategy where we identify individuals with severe ICI-myocarditis by also screening for and managing concomitant respiratory muscle involvement with mechanical ventilation and treating these individuals with high dose CTLA4-fusion protein abatacept with CD86RO monitoring and the Janus-kinase inhibitor ruxolitinib. We applied this strategy to 30 consecutive patients with ICI-myocarditis. By comparison, we also described a cohort of 10 patients seen previously where patients underwent usual recommended care with initiation of corticosteroids and addition of a secondary immunosuppressive therapy.

Results.

Study Cohort.

Of the 69 patients consecutively admitted for suspicion of ICI-myocarditis, 40 were confirmed as definite cases and were included in this report (**Figure 1** for flow-chart, **Table 1** for demographics & **Supplementary Table 1** for diagnostic certainty criteria). These patients were analyzed as the first 10 (quartile 1, Q1, admitted 05/2018-03/2020) treated as per current expert consensus guidelines starting with high dose corticosteroids boluses followed by second lines agents in case of cortico-resistance (16) versus the subsequent 30 (Q2-4, 03/2020-08/2021) treated with a mechanism-based approach. The mechanism-based approach included prompt use of high dose abatacept with real-time CD86RO monitoring, ruxolitinib, lower doses of corticosteroids, and systematic screening for and early management of concomitant respiratory muscle failure. The median age of the overall cohort was 72 [IQR=62,79]years, 58% were male; the most represented cancers were lung (9/40, 23%), skin (9/40, 23%) and genitourinary cancers (10/40, 25%). A majority of patients (30/40, 75%) developed severe (grade≥3) myotoxicity (**Table 2** and **Figure 2** for details concerning severity features of these patients & **Supplementary Tables 2-5** for detailed severity adjudication criteria). During the course of the disease, all patients had increased troponin-T (**Figure 2**); most (34/40, 85%) developed abnormal ECG features and 9/40(23%) developed severe systolic cardiac dysfunction (grade≥3). A total of 13% (5/40) required inotropic agents or extra-corporeal hemodynamic support. At least one cMRI examination (median/patient: 2[1-3]) supported the diagnosis in 26/35 (74%) (**Table-1** for results and **Supplementary Table 1** for cMRI diagnostic criteria; 5 patients died prior to cMRI or refused it). Cardiac and muscular biopsies supported the ICI-myotoxicity diagnosis in 24/32 (75%; 8 patients died prior to cardiac biopsy or refused it) and 36/40 (90%), respectively (**Table 1** for results and **Supplementary Table 1** for pathology criteria). Cardiac and muscular histopathology findings consistently showed T-cell and macrophage infiltration with associated myocyte necrosis (**Figure 3**). A total of 12/40 (30%) developed ventricular tachycardias (6/12, 50% sustained) and 9/40 (23%) developed severe conduction disorders (7 complete atrioventricular block, and 2 sinus node dysfunction requiring pacemaker implantation). Respiratory muscle involvement was present in 27/38 cases

(71%; 2 patients in Q1 died prior to evaluation) with specific evidence for diaphragmatic involvement in 22/38 cases (**Supplementary Table 3** for the detailed framework used to evaluate the global respiratory muscle and more specifically the diaphragm function). Respiratory muscle involvement was severe and required mechanical ventilation in over a third of patients (15/38) (**Table 1**). Electromyogram showed a myopathic pattern in half (19/37; 3 died before evaluation) of patients with no associated neuromuscular junction disorder (0/28 abnormal repetitive nerve stimulation test) despite clinical features of myasthenia-gravis (**Table 1**). Acetylcholine receptor antibodies were positive (>0.5nmol/L) in 8/40(20%), of which 5/5(100%) were previously known abnormal before initiation of ICI. Anti-muscle specific kinase antibodies were negative in all patients. In the 4 patients autopsied during the index hospitalization for ICI-myotoxicity, myocarditis and diaphragmatic myositis was severe, associated with lesions in peripheral muscles (**Figure 3**).

Cardio-myotoxicities outcomes with evolving management protocol.

The overall clinical demographic and diagnostic characteristics of patients in Q1 vs. Q2-4 were similar (**Table 1**) with no difference in peak cardiac troponin-T reached and in the different myotoxicity severity features studied (arrhythmia, cardiac and respiratory muscle dysfunction) upon presentation or during follow-up (**Table 2 & Figure 2**). In Q1, all patients were treated with corticosteroids (≥500mg/day intravenous methylprednisolone pulse ≥2days in 9/10(90%)) started within 2[0-4]days of presentation. 8/10 patients did not respond to corticosteroids ("cortico-resistant") and subsequently received plasmapheresis (2-5 cycles, n=8), low-dose abatacept (n=7), or mycophenolate-mofetil (n=4; time to start from presentation and dose are detailed in **Supplementary Table 6** and **Supplementary Figure 1**). ICI-myotoxicity related mortality was 60% (6/10) in Q1, with deaths due to cardiogenic shock or respiratory muscle failure (n=3 each). Among the first 10 patients, the diagnosis of respiratory muscle involvement was confirmed on chart review in 6/8 (75%). From Q1, we also identified that plasmapheresis partially cleared ICI blood levels (**Supplementary Figure 2**), but identification of PD(L)1 expression on T-cells was markedly delayed to few months after pheresis (**Figure 4**). We also inferred that plasmapheresis would clear abatacept (an example provided in **Figure 5**), so we delayed using the drug after plasmapheresis.(1) Moreover, in the first 10 patients, we found that the initial abatacept

dosing strategy did not improve outcome (60% of ICI-related mortality in Q1). Indeed, even with higher abatacept doses used subsequently in Q2-4, CD86RO peak levels were often below the objective of CD86RO≥80% and we identified that CD86RO varied dose-dependently after abatacept injections (**Figure 6**).

With the above information from Q1 patients, we modified treatment and monitoring strategy for patients in Q2-4. We stopped performing plasmapheresis in severe cases instead opting for initiation of higher dose abatacept if grade≥3 (severe) myotoxicity criteria were met. The abatacept starting dose was increased to ~20mg/kg on days 0, 5, and 14 and the total dose administered in the first 2 weeks was 60 [53-65]mg/kg in Q2-4 vs 41 [24-60]mg/kg in Q1 (p=0.01 for Q1 vs. Q2-4, **Supplementary Table 6** for evolution of abatacept dose used per specific quartile). In severe cases in Q2-4 (22/30 patients), we added ruxolitinib to abatacept and corticosteroids based on pre-clinical and translational studies outlined below, as well as given rapid onset of action of ruxolitinib (in contrast to abatacept which has delayed onset of action). Ruxolitinib was used in 0/8 of severe cases in Q1 vs. 17/22, 77% in Q2-4 (p=0.0002). In Q2-4, abatacept was used in all 22 severe cases. In Q2-4, we used lower concomitant doses of corticosteroids seeking for less related adverse events vs. Q1 (intravenous methylprednisolone equivalent pulse ≥500mg/day in 13/30, 43% in Q2-4 vs. 9/10, 90% in Q1, p=0.01; 155 [122-223]mg of mean daily dose in the 1st month of treatment in Q1 vs. 96[21-156] mg/day in Q2-4, p=0.02; **Supplementary Table 6** for evolution of treatment modalities per specific quartile). The median time between presentation, appearance of grade≥3 (severe) ICI-myotoxicity criteria, and use of immunosuppressants are shown in **Supplementary Figure 1** and **Supplementary Table 6**. Frequencies of side effects observed on immunosuppressants including infections are detailed in **Supplementary Table 6**. In Q2-4, all patients were screened for respiratory muscle involvement for a decision concerning ventilator indication and management. While the proportion of severe cases (grade≥3) was comparable in Q1 (8/10, 80%) and Q2-4 (22/30, 73%, p=0.67), the combined pharmacotherapeutic and ventilatory strategy was associated with a decrease in ICI-related myotoxicity death from 6/10 (60%) in Q1 to 1/30 (3%) in Q2-4 (p<0.0001). Restricting analysis to severe (grade≥3) cases, results were similar with 6/8 (80%) ICI-related myotoxicity death in Q1 vs. 1/22 (5%) in Q2-4 (p<0.0001). With the use of screening for respiratory muscle failure in Q2-Q4, 10/30 (30%)

were found eligible for elective ventilation and this was started in all but one who declined intubation (and who was the only death in Q2-Q4), and one with hepatic cancer who died of decompensated cirrhosis before ventilation was started. In these 8 ventilated patients (details on the modality of ventilation in **Supplementary Figure 1**), recovery was complete in 6/8 (median weaning time=17[2-111]days) and 2/8 were recovering (weaned from diurnal ventilation) being on residual nocturnal ventilation at 6month follow-up.

There were deaths due to other causes (**Figure 1**) including covid-19 (in Q2-4) and sepsis (Q1). All-cause mortality at 3 months was 6/10 (60%) in Q1 and dropped to 7/30 (23%, p=0.03) in Q2-4; the corresponding figures at 6 months were 7/10 (70%) vs. 9/30 (30%, p=0.03). Restricting analysis of all-cause mortality to severe cases showed similar results at 3 months (6/8, 75% in Q1 vs. 5/22, 23%; p=0.009) and 6 months (7/8, 88% in Q1 vs. 7/22, 32%; p=0.007). Median overall survival 6 months after presentation for ICI-myocarditis was not reached in ICI-myotoxicity survivor's (n=33) vs. 0.7 months in those dead from ICI-myotoxicity (n=7, p<0.001, **Figure 7**). Among patients surviving ICI-related myotoxicity, 82% had stable disease or a partial response and median PFS was 5.7 months (**Figure 7**). Best change from baseline in tumor burden as a function of their cancer type and immunosuppressants received are shown in **Figure 7E** & **7F**, respectively. Pacemakers were placed in 8 patients and in 5/8 (63%), the conduction disorder resolved after 8[2-22] days. Three patients were still pacemaker-dependent at 1year follow-up; two were alive and the other died of COVID-19 with complete destruction of the sinus node at autopsy (**Figure 3F**).

The Q2-4 group included 4 patients with asymptomatic myocarditis with grade-1 ICI-myotoxicity criteria, diagnosed by abnormal Troponin-T but with no concomitant symptomatic irAE; there was a mild increase of peak troponin-T of 5[3-8] fold-change above upper reference limit vs. 116[60-223] in the other 36 (p=0.0002, **Figure 1**). In these 4 patients, immunosuppressant drugs were not used but ICI were withheld. One such patient was re-challenged with ICI 2 months after the first episode but developed severe hepatitis(16) leading to permanent ICI discontinuation.

Rationale for JAK-STAT pathway inhibition to treat ICI-myotoxicity.

To elucidate underlying signaling mechanisms of ICI-myocarditis, we have utilized a genetic mice model (*ctla4*$^{+/-}$ *pd1*$^{-/-}$) of ICI-myocarditis, which recapitulates the clinical and pathological features seen in patients; and which we initially used to demonstrate the biological plausibility and efficacy of abatacept.(19) Despite efficacy, abatacept onset was slow with minimal clearance of cardiac immune infiltrates after 2 weeks of treatment with abatacept in mice.(19) We therefore felt that abatacept would need to be combined with an immunosuppressive with a shorter onset of action. In parallel, we performed bulk RNA sequencing assessing transcriptomics and pathways affected in our mouse model. We compared these identified pathways in mice to human tissue after performing bulk RNA-sequencing from endomyocardial biopsies of patients with ICI-myocarditis compared to ICI treated patients with no myocarditis.(28) In ICI-myocarditis mice (*ctla4*$^{+/-}$*pd1*$^{-/-}$), bulk RNA sequencing showed very distinct affected pathways in ICI-myocarditis mice compared to unaffected control mice (*ctla4*$^{+/+}$ *pd1*$^{-/-}$) (**Figure 6A**). JAK-STAT signaling was especially upregulated with *Jak2* being the most significantly upregulated gene among the *Jak* family, and *Stat1* and *Stat4* were the most significantly upregulated genes among the *Stat* family (**Figure 6B**). *Interferon-gamma*/*Jak2*/*Stat1* signaling, *Interleukin12*/*Jak2*/*Stat4* signaling, and *Interleukin6*/*Jak2*/*Stat3* signaling were the most significantly upregulated signaling pathways in ICI-myocarditis mice compared to unaffected control mice (**Figure 6C**). Bulk RNA-sequencing from patients also indicated that *Jak2* was the only significantly upregulated gene in the *JAK* family in patients with ICI-myocarditis (n=9), compared to ICI-treated patients without evidence of myocarditis (n=4) (**Figure 6D**). These findings from both mice and human data support the potential beneficial effect of ruxolitinib (a JAK1/JAK2 inhibitor) in ICI-myocarditis."

Discussion.

In this study, we showed that prompt high-dose abatacept with real-time assessment of CD86RO immuno-monitoring combined with ruxolitinib, corticosteroids, and active management of respiratory muscle involvement was associated with a decrease in ICI-myotoxicity related death among ICI-myocarditis patients. With this strategy, ICI-myotoxicity related mortality decreased to ~3%, from historical controls (20-60% in other published cohorts worldwide with ICI-myocarditis) as well as the first 10 cases in our patient cohort (60% in our Q1 cases) who did not undergo screening and treatment with this strategy.(2-4,8,29,30) While our study is not a clinical trial, our results may provide a promising platform by which to best treat the growing population that presents with fulminant ICI-myocarditis, with a mechanism-based and personalized assessment of drug receptor occupancy. The concept of abatacept use for ICI-myocarditis initially came from successful treatment in a genetic mouse model with subsequent clinical case reports.(19,20) Our study presents a comprehensive approach to treatment of these patients with attention to extra-cardiac myotoxicity associated with disease and attention to abatacept pharmacodynamics, associated with ruxolitinib use.

One key element for improved care of ICI-myocarditis has been our recognition that skeletal muscle involvement is near-universal (95% abnormal muscular biopsy). With a very high frequency of respiratory muscle involvement comparable to that found in other types of systemic myositis,(31) screening for (serial arterial blood gases) and management of respiratory muscle involvement appeared critical in avoiding life-threatening hypoventilation. As T-cells and macrophages are critical in the development of ICI-myocarditis and ICI-myositis, optimizing immunossupressant therapy was also a critical advance in our approach.(1,19,20) Abatacept antagonizes the activation of ICI pathways through blockade of T-cells activation by antigen-presenting-cells (ie blocking the interaction between CD86 on monocytes and CD28 on T-cells). (1,24-27,32) Moreover, using translational approaches in mice and human, we were able to show that JAK2 signaling pathways were specifically activated in the heart of ICI-myocarditis mice and patients (namely *Interferon-gamma/Jak2/Stat1*; *Interleukin12/Jak2/Stat4*; and *Interleukin6/Jak2/Stat3;* **Figure 8***)*. These findings

supported the specific use of ruxolitinib (a JAK1, JAK 2 inhibitor notably blocking interleukin-6 and Interferon-gamma cytokine pathways) among available JAK inhibitors previously proposed in the treatment of other types of irAE such as ICI-colitis.(33-36) More research is needed to further decipher the full mechanistic spectrum of the potential beneficial effects of ruxolitinib to treat ICI-myotoxicity, including its potential to decrease the antigenic presentation by muscle cells (making them harder targets) or to block some of the pro-apoptotic functions of Interferon-gamma.(37,38)

All 8 patients in whom we implemented early mechanical ventilation for respiratory muscle failure had near complete recovery, to the point of full weaning in 6 cases and weaning during the day in 2 cases. This contrasts with the experience presented in a very similar cohort of severe ICI-myotoxicity,(14) in which 8/12 (67%) patients who developed respiratory failure attributable to respiratory muscle myositis died despite use of very high-dose corticosteroids, plasmapheresis, intravenous immunoglobulin and rituximab.(14) Notably, the time to recovery of respiratory muscle failure in our cohort varied from a few days to several months, apparently depending on severity of initial presentation. Very slow recovery of respiratory muscle function after control of the causative insult has been well described in other neuro-myopathies affecting respiratory muscles.(39,40) In the case of ICI-myotoxicities, the concomitant use of high-dose corticosteroids favoring sarcopenia may also interfere deleteriously with muscular recovery.(41,42)

Several limitations of our analysis need to be recognized. As any non-randomized observational study, there is a risk of unaccounted bias between compared groups. In our study, we did not find any difference between quartiles in known ICI-myotoxicity severity criteria including peak troponin levels, proportion of patients treated by combination ICI therapy or presenting with severe arrhythmias, heart and respiratory muscle failure (**Table 2**).(10) Our population was too small to perform ancillary analysis better adjusted on the dose of corticosteroids received, or any other subtlety related to the type of anticancer treatment or immunosuppressant regimen received. Indeed, in Q2-4, both high-dose abatacept and addition of ruxolitinib were started precluding comparison of each treatment modality individually. Abatacept dose used within the 2 first weeks of treatment start in Q2-4 was higher vs. Q1 (~60 vs. 40mg/kg, respectively), but it has to be

acknowledged that both these doses are much higher as compared to the intravenous loading dose used in abatacept's approved indication (10mg/kg every 2 weeks in rheumatoid arthritis).(1) Indeed, these doses are closer to belatacept loading dose equivalent given in graft rejection prophylaxis.(1)

A major challenge to consider while treating patient with severe irAE is how to mitigate symptoms and mortality risk while preserving anti-tumor beneficial effects. In our cohort, abatacept and ruxolitinib were used only over a short period (~1-2 months) of active treatment to achieve resolution of severity criteria, and this also limited the corticosteroid dose. To date, it is unclear to what extent the approach we used to treat ICI-myotoxicities altered ICI anticancer efficacy or would be efficient in other life-threatening irAE.(2) Of note, it is also important to highlight that most irAE toxicities are not life-threatening and can be even detected while infra-clinical by active screening strategies (e.g., by systematic troponin surveillance).(10) These low grades irAE would not require the same immunosuppressive strategy (if any) as life-threatening irAE.(16) The PFS estimate in our cohort (~6months) is unique since most previous ICI-myocarditis cohorts focused on describing the deadly cardiac outcomes and did not report cancer response. The variety of cancers in our cohort (mainly metastatic melanoma, lung, and kidney cancers) precluded us from performing reliable comparison to expected PFS in historical cohorts. However, median PFS in ICI clinical trials focusing on these latter cancers were consistently below 6 months (3-5 months).(1) Altogether, our results are promising and should guide further research assessing the question of the optimal drug mix, dosage and duration to be used to preserve ICI therapeutic effect while treating a severe irAE, the subject of further ongoing clinical study (*NCT05195645*). Comparison to other alternative pharmacological approaches also targeting T-cells (e.g anti-thymoglobulin, alemtuzumab, anti-calcineurin drugs) and proposed in current treatment guidelines for irAE also deserve further assessment.(16) Meanwhile, the findings reported here justify a prompt referral to expert centers, able to evaluated the severity of patients notably by providing a systematic assessment and very close monitoring of respiratory muscle function in patients with ICI-myocarditis, to avoid missing life-saving indications for ventilatory assistance.

Methods.

Study Cohort. This prospective single-center cohort included 40 consecutive patients with definite ICI-myocarditis admitted to our cardio-oncology unit (Pitié-Salpétrière, Paris, France) among 69 evaluated for suspected ICI-related myocarditis between 10/05/2018 and 08/18/2021 (Flow chart in **Figure 1**). ICI-related myotoxicity was confirmed by endomyocardial or muscle biopsies in all patients. Diagnostic certainty for ICI-myocarditis was determined based on modified Bonaca et. al criteria (**Supplementary Table 1**).(11) The general diagnostic work-up strategy upon ICI-myocarditis suspicion is detailed in **Supplementary Table 2**. A diagnosis of respiratory muscle involvement was established using the 2019 European Respiratory Society statement.(43) All these patients were included in the *MASC* (Myositis, DNA, Serum, Cells: Clinical Database and Biobank of Patients With Inflammatory Myopathies) prospective cohort (ethical approval CPP#2013 Ile de France VI; *NCT04637672*). Patients were treated after providing their written consent for compassionate use for abatacept and ruxolitinib. This study was conducted in accordance with Declaration of Helsinki ethical guidelines. Follow-up exceeded 6 months.

Adjudications of events. Patients' charts were reviewed by two respiratory physicians to evaluate respiratory muscle dysfunction and its severity using a multi-parametric approach detailed in **Supplementary Table 3**.(43) Cardiac and skeletal muscle involvement (**Supplementary Table 4** & **Supplementary Table 5**) and oncological status (progression free survival, PFS) were prospectively assessed and graded (adapted from current guidelines) by two cardio-oncologists, a medical oncologist, and a radiologist.(16,44) Cardiac involvement was evaluated by cardiac MRI, endomyocardial biopsy, coronary angiography, echocardiography, electrocardiography and Troponin-T (ultrasensitive assay, Elecsys ROCHE Diagnostics®) monitoring. Skeletal muscle involvement was evaluated by peripheral muscle and diaphragmatic MRI, muscular biopsy, electromyogram, diaphragmatic echography and pulmonary functional test specifically seeking for respiratory muscle dysfunction (**Supplementary Table 3**). All causes of death were evaluated by three independent investigators. Autopsies were performed to determine exact cause of death, if family consented. ICI-related myotoxicities were considered severe (grade≥3) if any of the following was present: severe arrhythmias

(defined as appearance of ventricular tachyarrhythmias or high-degree atrioventricular block or sinus node dysfunction), heart failure (defined as heart failure symptoms requiring intravenous diuretics or inotropes or hemodynamic support), respiratory muscle failure leading to hypoventilation, or deterioration of bio-clinical status despite corticosteroids (**Supplementary Table 4** & **Supplementary Table 5**).(16,44)

Therapeutic strategy. The first 10 patients (starting in 2018 until March 2020) were treated with high dose boluses of corticosteroids regardless of symptoms.(16,44) In severe cases (grade≥3, defined above), plasmapheresis, mycophenolate-mofetil and abatacept (~10mg/kg per injection approximately every 2 weeks) were used, according to current guidelines.(16,44) After the first 10 patients (March 2020 to August 2021), our strategy was modified to include systematic screening in these ICI-myocarditis patients for and management of concomitant respiratory muscle failure (myositis) including serial and repeated arterial blood gases to identify alveolar hypoventilation – increase carbon dioxide partial pressure, $PaCO_2$– (**Supplementary Table 3**) and in severe cases: (1) prompt initiation of higher dose abatacept (≈20mg/kg, 3 doses within the first 2 weeks of treatment start) with dose-adjustment based on real-time assessment of CD86RO targeting peak value of CD86RO≥80% within 72hours of abatacept and residual CD86RO≥50% (**Figure 5** and **Supplementary Figure 1** for examples) until resolution of myotoxicity severity to grade≤2 (**Figure 2** & **Supplementary Table 5** for details concerning severity grading features); (2) addition of ruxolitinib used with abatacept; and (3) decrease in corticosteroids dose used to avoid associated side-effects (**Supplementary Table 6** for details concerning reporting of side-effects). (16,21,44) Also, starting from March 2020 until August 2021, asymptomatic cases detected by screening (Grade-1, **Figure 2** & **Supplementary Table 5**) were monitored after withholding ICI with no systematic immunossupressant treatment.(16,45,46) Summary of our general therapeutic management starting March 2020 depending on grade of severity of ICI-myotoxicity is in **Supplementary Table 5**.

Immune-monitoring. Details concerning the methodology for profiling of immune-checkpoint proteins on peripheral blood mononuclear cells (CD86RO on monocytes, PD(L)1 expression on T-cells) and monitoring of abatacept or ICI plasma levels are detailed in **Figure 5** and **Appendix-Methods**.(47)

Statistics. Quantitative and qualitative data are expressed as median [interquartile-range, IQR] and n(%). Their comparison was performed by Mann-Whitney or Kruskal-Wallis tests (when comparing quantitative variables between two groups or more, respectively) and χ2-tests for comparison of qualitative variables (including trends by quartiles when appropriate). Correlation between quantitative variables were assessed by Spearman's correlation. P<0.05 was deemed significant.

JAK-STAT pathway translational studies.

RNA-isolation and sequencing using mice cardiac tissues

ICI-myocarditis mice (n=3, *ctla4+/- pd-1-/-)* were compared to unaffected control mice (n=4, *ctla4+/+ pd-1-/-).(19)* Flash-frozen mouse tissue (cardiac ventricle) was homogenized using a TissueLyser II (Qiagen) for 2 min at 30 Hz. RNA was collected from dissociated tissue using Qiagen RNA Kit (Catalog#, 74136). Libraries were prepared using Illumina TruSeq Stranded Total RNA Kit (Illumina, San Diego, CA, USA). Sequencing was performed as paired-end sequencing, with a read length of 150 bps on the Illumina NovaSeq 6000 platform.

Bioinformatical analysis using human cardiac tissues

We used previously published bulk RNA-sequencing data from endomyocardial biopsies of patients with ICI-myocarditis (*n*=9) compared with ICI-treated patients without myocarditis (*n*=4) included at Heidelberg (Germany).(28) These data were obtained from the EBI ArrayExpress Database, with accession number E-MTAB-8867. The raw data files were aligned to the mouse or human genome using the RNA STAR software (Version 2.7.3). Reads (reads per kilobase million) were extracted from the mapped files using the Rsubread Bioconductor package (Version 3.1). Differential gene expression was calculated using the DESeq2 algorithms (European Molecular Biology Laboratory, Heidelberg, Germany) with a false discovery rate <0.05. For visualizations, we used the ggplot2 and heatmap3 R packages.

References.

1. Geraud A, Gougis P, Vozy A, Anquetil C, Allenbach Y, Romano E*, et al.* Clinical Pharmacology and Interplay of Immune Checkpoint Agents: A Yin-Yang Balance. Annu Rev Pharmacol Toxicol **2021**;61:85-112 doi 10.1146/annurev-pharmtox-022820-093805.
2. Wang DY, Salem JE, Cohen JV, Chandra S, Menzer C, Ye F*, et al.* Fatal Toxic Effects Associated With Immune Checkpoint Inhibitors: A Systematic Review and Meta-analysis. JAMA Oncol **2018**;4(12):1721-8 doi 10.1001/jamaoncol.2018.3923.
3. Salem JE, Manouchehri A, Moey M, Lebrun-Vignes B, Bastarache L, Pariente A*, et al.* Cardiovascular toxicities associated with immune checkpoint inhibitors: an observational, retrospective, pharmacovigilance study. Lancet Oncol **2018**;19(12):1579-89 doi 10.1016/S1470-2045(18)30608-9.
4. Nguyen LS, Cooper LT, Kerneis M, Funck-Brentano C, Silvain J, Brechot N*, et al.* Systematic analysis of drug-associated myocarditis reported in the World Health Organization pharmacovigilance database. Nat Commun **2022**;13(1):25 doi 10.1038/s41467-021-27631-8.
5. Allenbach Y, Anquetil C, Manouchehri A, Benveniste O, Lambotte O, Lebrun-Vignes B*, et al.* Immune checkpoint inhibitor-induced myositis, the earliest and most lethal complication among rheumatic and musculoskeletal toxicities. Autoimmun Rev **2020**;19(8):102586 doi 10.1016/j.autrev.2020.102586.
6. Anquetil C, Salem JE, Lebrun-Vignes B, Johnson DB, Mammen AL, Stenzel W*, et al.* Immune Checkpoint Inhibitor-Associated Myositis: Expanding the Spectrum of Cardiac Complications of the Immunotherapy Revolution. Circulation **2018**;138(7):743-5 doi 10.1161/CIRCULATIONAHA.118.035898.
7. Johnson DB, Balko JM, Compton ML, Chalkias S, Gorham J, Xu Y*, et al.* Fulminant Myocarditis with Combination Immune Checkpoint Blockade. N Engl J Med **2016**;375(18):1749-55 doi 10.1056/NEJMoa1609214.
8. Power JR, Alexandre J, Choudhary A, Ozbay B, Hayek S, Asnani A*, et al.* Electrocardiographic Manifestations of Immune Checkpoint Inhibitor Myocarditis. Circulation **2021**;144(18):1521-3 doi 10.1161/CIRCULATIONAHA.121.055816.
9. Power JR, Alexandre J, Choudhary A, Ozbay B, Hayek SS, Asnani A*, et al.* Association of early electrical changes with cardiovascular outcomes in immune checkpoint inhibitor myocarditis. Arch Cardiovasc Dis **2022**;115(5):315-30 doi 10.1016/j.acvd.2022.03.003.
10. Lehmann LH, Cautela J, Palaskas N, Baik AH, Meijers WC, Allenbach Y*, et al.* Clinical Strategy for the Diagnosis and Treatment of Immune Checkpoint Inhibitor-Associated Myocarditis: A Narrative Review. JAMA Cardiol **2021**;6(11):1329-37 doi 10.1001/jamacardio.2021.2241.
11. Bonaca MP, Olenchock BA, Salem JE, Wiviott SD, Ederhy S, Cohen A*, et al.* Myocarditis in the Setting of Cancer Therapeutics: Proposed Case Definitions for Emerging Clinical Syndromes in Cardio-Oncology. Circulation **2019**;140(2):80-91 doi 10.1161/CIRCULATIONAHA.118.034497.
12. Zhang L, Awadalla M, Mahmood SS, Nohria A, Hassan MZO, Thuny F*, et al.* Cardiovascular magnetic resonance in immune checkpoint inhibitor-associated myocarditis. Eur Heart J **2020**;41(18):1733-43 doi 10.1093/eurheartj/ehaa051.
13. Ederhy S, Salem JE, Dercle L, Hasan AS, Chauvet-Droit M, Nhan P*, et al.* Role of Cardiac Imaging in the Diagnosis of Immune Checkpoints Inhibitors Related Myocarditis. Front Oncol **2021**;11:640985 doi 10.3389/fonc.2021.640985.
14. Aldrich J, Pundole X, Tummala S, Palaskas N, Andersen CR, Shoukier M*, et al.* Inflammatory Myositis in Cancer Patients Receiving Immune Checkpoint Inhibitors. Arthritis Rheumatol **2021**;73(5):866-74 doi 10.1002/art.41604.
15. Axelrod ML, Meijers WC, Screever EM, Qin J, Carroll MG, Sun X*, et al.* T cells specific for alpha-myosin drive immunotherapy-related myocarditis. Nature **2022**;611(7937):818-26 doi 10.1038/s41586-022-05432-3.

16. Schneider BJ, Naidoo J, Santomasso BD, Lacchetti C, Adkins S, Anadkat M*, et al.* Management of Immune-Related Adverse Events in Patients Treated With Immune Checkpoint Inhibitor Therapy: ASCO Guideline Update. J Clin Oncol **2021**;39(36):4073-126 doi 10.1200/JCO.21.01440.
17. Wang C, Lin J, Wang Y, Hsi DH, Chen J, Liu T*, et al.* Case Series of Steroid-Resistant Immune Checkpoint Inhibitor Associated Myocarditis: A Comparative Analysis of Corticosteroid and Tofacitinib Treatment. Front Pharmacol **2021**;12:770631 doi 10.3389/fphar.2021.770631.
18. Power J, Meijers W, Fenioux C, Tamura Y, Asnani A, Alexandre J*, et al.* Predictors of steroid-refractory immune checkpoint inhibitor associated myocarditis. European Heart Journal **2020**;41(Supplement_2) doi 10.1093/ehjci/ehaa946.3272.
19. Wei SC, Meijers WC, Axelrod ML, Anang NAS, Screever EM, Wescott EC*, et al.* A Genetic Mouse Model Recapitulates Immune Checkpoint Inhibitor-Associated Myocarditis and Supports a Mechanism-Based Therapeutic Intervention. Cancer Discov **2021**;11(3):614-25 doi 10.1158/2159-8290.CD-20-0856.
20. Salem JE, Allenbach Y, Vozy A, Brechot N, Johnson DB, Moslehi JJ*, et al.* Abatacept for Severe Immune Checkpoint Inhibitor-Associated Myocarditis. N Engl J Med **2019**;380(24):2377-9 doi 10.1056/NEJMc1901677.
21. Nguyen LS, Bretagne M, Arrondeau J, Zahr N, Ederhy S, Abbar B*, et al.* Reversal of immune-checkpoint inhibitor fulminant myocarditis using personalized-dose-adjusted abatacept and ruxolitinib: proof of concept. J Immunother Cancer **2022**;10(4) doi 10.1136/jitc-2022-004699.
22. Latek R, Fleener C, Lamian V, Kulbokas E, 3rd, Davis PM, Suchard SJ*, et al.* Assessment of belatacept-mediated costimulation blockade through evaluation of CD80/86-receptor saturation. Transplantation **2009**;87(6):926-33 doi 10.1097/TP.0b013e31819b5a58.
23. Zhou Z, Shen J, Hong Y, Kaul S, Pfister M, Roy A. Time-varying belatacept exposure and its relationship to efficacy/safety responses in kidney-transplant recipients. Clin Pharmacol Ther **2012**;92(2):251-7 doi 10.1038/clpt.2012.84.
24. Zeiser R, von Bubnoff N, Butler J, Mohty M, Niederwieser D, Or R*, et al.* Ruxolitinib for Glucocorticoid-Refractory Acute Graft-versus-Host Disease. N Engl J Med **2020**;382(19):1800-10 doi 10.1056/NEJMoa1917635.
25. Lescoat A, Lelong M, Jeljeli M, Piquet-Pellorce C, Morzadec C, Ballerie A*, et al.* Combined anti-fibrotic and anti-inflammatory properties of JAK-inhibitors on macrophages in vitro and in vivo: Perspectives for scleroderma-associated interstitial lung disease. Biochem Pharmacol **2020**;178:114103 doi 10.1016/j.bcp.2020.114103.
26. Deszo EL, Brake DK, Kelley KW, Freund GG. IL-4-dependent CD86 expression requires JAK/STAT6 activation and is negatively regulated by PKCδ. Cellular Signalling **2004**;16(2):271-80 doi 10.1016/s0898-6568(03)00137-2.
27. Kubo S, Yamaoka K, Kondo M, Yamagata K, Zhao J, Iwata S*, et al.* The JAK inhibitor, tofacitinib, reduces the T cell stimulatory capacity of human monocyte-derived dendritic cells. Ann Rheum Dis **2014**;73(12):2192-8 doi 10.1136/annrheumdis-2013-203756.
28. Finke D, Heckmann MB, Salatzki J, Riffel J, Herpel E, Heinzerling LM*, et al.* Comparative Transcriptomics of Immune Checkpoint Inhibitor Myocarditis Identifies Guanylate Binding Protein 5 and 6 Dysregulation. Cancers (Basel) **2021**;13(10) doi 10.3390/cancers13102498.
29. Mahmood SS, Fradley MG, Cohen JV, Nohria A, Reynolds KL, Heinzerling LM*, et al.* Myocarditis in Patients Treated With Immune Checkpoint Inhibitors. J Am Coll Cardiol **2018**;71(16):1755-64 doi 10.1016/j.jacc.2018.02.037.
30. Nowatzke J, Guedeney P, Palaskas N, Lehmann L, Ederhy S, Zhu H*, et al.* Coronary artery disease and revascularization associated with immune checkpoint blocker myocarditis: Report from an international registry. Eur J Cancer **2022** doi 10.1016/j.ejca.2022.07.018.
31. Teixeira A, Cherin P, Demoule A, Levy-Soussan M, Straus C, Verin E*, et al.* Diaphragmatic dysfunction in patients with idiopathic inflammatory myopathies. Neuromuscul Disord **2005**;15(1):32-9 doi 10.1016/j.nmd.2004.09.006.

32. Chen C-Y, Chiu C-F, Bai L-Y. Treatment of pembrolizumab-induced cutaneous lesions with ruxolitinib. European Journal of Cancer **2019**;113:69-71 doi 10.1016/j.ejca.2019.03.016.
33. Bishu S, Melia J, Sharfman W, Lao CD, Fecher LA, Higgins PDR. Efficacy and Outcome of Tofacitinib in Immune checkpoint Inhibitor Colitis. Gastroenterology **2021**;160(3):932-4 e3 doi 10.1053/j.gastro.2020.10.029.
34. Sasson SC, Slevin SM, Cheung VTF, Nassiri I, Olsson-Brown A, Fryer E*, et al.* Interferon-Gamma-Producing CD8(+) Tissue Resident Memory T Cells Are a Targetable Hallmark of Immune Checkpoint Inhibitor-Colitis. Gastroenterology **2021**;161(4):1229-44 e9 doi 10.1053/j.gastro.2021.06.025.
35. Luoma AM, Suo S, Williams HL, Sharova T, Sullivan K, Manos M*, et al.* Molecular Pathways of Colon Inflammation Induced by Cancer Immunotherapy. Cell **2020**;182(3):655-71 e22 doi 10.1016/j.cell.2020.06.001.
36. Yeleswaram S, Smith P, Burn T, Covington M, Juvekar A, Li Y*, et al.* Inhibition of cytokine signaling by ruxolitinib and implications for COVID-19 treatment. Clin Immunol **2020**;218:108517 doi 10.1016/j.clim.2020.108517.
37. Heine A, Held SA, Daecke SN, Wallner S, Yajnanarayana SP, Kurts C*, et al.* The JAK-inhibitor ruxolitinib impairs dendritic cell function in vitro and in vivo. Blood **2013**;122(7):1192-202 doi 10.1182/blood-2013-03-484642.
38. Albeituni S, Verbist KC, Tedrick PE, Tillman H, Picarsic J, Bassett R*, et al.* Mechanisms of action of ruxolitinib in murine models of hemophagocytic lymphohistiocytosis. Blood **2019**;134(2):147-59 doi 10.1182/blood.2019000761.
39. Hughes PD, Polkey MI, Moxham J, Green M. Long-term recovery of diaphragm strength in neuralgic amyotrophy. Eur Respir J **1999**;13(2):379-84 doi 10.1183/09031936.99.13237999.
40. Rice BL, Ashton RW, Wang XF, Shook SJ, Mireles-Cabodevila E, Aboussouan LS. Modeling of Lung Function Recovery in Neuralgic Amyotrophy With Diaphragm Impairment. Respir Care **2017**;62(10):1269-76 doi 10.4187/respcare.05568.
41. Ferguson GT, Irvin CG, Cherniack RM. Effect of corticosteroids on respiratory muscle histopathology. Am Rev Respir Dis **1990**;142(5):1047-52 doi 10.1164/ajrccm/142.5.1047.
42. Weiner P, Azgad Y, Weiner M. The effect of corticosteroids on inspiratory muscle performance in humans. Chest **1993**;104(6):1788-91 doi 10.1378/chest.104.6.1788.
43. Laveneziana P, Albuquerque A, Aliverti A, Babb T, Barreiro E, Dres M*, et al.* ERS statement on respiratory muscle testing at rest and during exercise. Eur Respir J **2019**;53(6) doi 10.1183/13993003.01214-2018.
44. Brahmer JR, Lacchetti C, Schneider BJ, Atkins MB, Brassil KJ, Caterino JM*, et al.* Management of Immune-Related Adverse Events in Patients Treated With Immune Checkpoint Inhibitor Therapy: American Society of Clinical Oncology Clinical Practice Guideline. J Clin Oncol **2018**;36(17):1714-68 doi 10.1200/JCO.2017.77.6385.
45. Palaskas NL, Segura A, Lelenwa L, Siddiqui BA, Subudhi SK, Lopez-Mattei J*, et al.* Immune checkpoint inhibitor myocarditis: elucidating the spectrum of disease through endomyocardial biopsy. Eur J Heart Fail **2021**;23(10):1725-35 doi 10.1002/ejhf.2265.
46. Ederhy S, Devos P, Pinna B, Funck-Brentano E, Abbar B, Fenioux C*, et al.* (18)F-fluorodeoxyglucose positron emission tomography/computed tomography imaging for the diagnosis of immune checkpoint inhibitor-associated myocarditis. Arch Cardiovasc Dis **2022**;115(2):114-6 doi 10.1016/j.acvd.2021.12.001.
47. Pitoiset F, Cassard L, El Soufi K, Boselli L, Grivel J, Roux A*, et al.* Deep phenotyping of immune cell populations by optimized and standardized flow cytometry analyses. Cytometry A **2018**;93(8):793-802 doi 10.1002/cyto.a.23570.
48. Eisenhauer EA, Therasse P, Bogaerts J, Schwartz LH, Sargent D, Ford R*, et al.* New response evaluation criteria in solid tumours: revised RECIST guideline (version 1.1). Eur J Cancer **2009**;45(2):228-47 doi 10.1016/j.ejca.2008.10.026.

Table 1. Demographics & diagnostic work-up of patients included by time period of inclusion

Dates of inclusion in the consecutive quartiles (months/years)	**Overall** 05/18 - 08/21	**Quartile 1** 05/18 - 03/20	**Quartile 2** 03/20 - 12/20	**Quartile 3** 12/20 - 04/21	**Quartile 4** 05/21-08/21	**p-value**
	n/N (%), or median [interquartile range as appropriate]					
Demographics						
Age, years	72 [62-79]	67 [61-77]	68 [51-79]	75 [68-84]	72 [64-75]	0.33
Sex, male (%)	23 (58%)	6 (60%)	6 (60%)	6 (60%)	5 (50%)	0.67
Body mass index, kg/m²	24 [22-27]	24 [19-26]	24 [21-29]	25 [20-26]	24 [22-29]	0.63
Time to onset after first ICI dose	33 [21-42]	32 [16-64]	34 [27-41]	28 [21-41]	34 [19-64]	0.97
- days	2 [1-3]	2 [1-4]	2 [1-2]	2 [1-2]	2 [1-3]	0.92
- number of doses						
Past medical history (%)						
- heart failure	2 (5%)	0 (0%)	2 (20%)	0 (0%)	0 (0%)	0.52
- hypertension	20 (50%)	4 (40%)	5 (50%)	5 (50%)	6 (60%)	0.40
- diabetes	7 (18%)	2 (20%)	1 (10%)	2 (20%)	2 (20%)	0.85
- dyslipidemia	8 (20%)	3 (30%)	2 (20%)	1 (10%)	2 (20%)	0.48
- auto-immune disease	7 (18%)	2 (20%)	2 (20%)	0 (0%)	3 (30%)	0.85
Cancer status (%)						
- metastatic	33 (83%)	8 (80%)	7 (70%)	9 (90%)	9 (90%)	0.91
Diagnostic work-up						
Cardiac symptoms						
- chest pain	11 (28%)	6 (60%)	3 (30%)	2 (20%)	0 (0%)	0.003
- syncope/faintness	7 (18%)	3 (30%)	1 (10%)	2 (20%)	1 (10%)	0.35
- dyspnea	24 (60%)	9 (90%)	5 (50%)	5 (50%)	5 (50%)	0.08
- palpitations	6 (15%)	2 (20%)	3 (30%)	1 (10%)	0 (0%)	0.11
Muscular symptoms						
- muscular pain or weakness	28 (70%)	8 (80%)	8 (80%)	8 (80%)	4 (40%)	0.06
- ptosis	16 (40%)	4 (40%)	5 (50%)	3 (30%)	4 (40%)	0.77
- diplopia	16 (40%)	5 (50%)	5 (50%)	2 (20%)	4 (40%)	0.39
- dysphagia	13 (33%)	5 (50%)	3 (30%)	2 (20%)	3 (30%)	0.29
- dysphonia	14 (35%)	4 (40%)	4 (40%)	2 (20%)	4 (40%)	0.77
Electrocardiogram abnormal	34 (85%)	9 (90%)	10 (100%)	8 (80%)	7 (70%)	0.11
Creatinine kinase abnormal	36 (90%)	9 (90%)	8 (80%)	9 (90%)	10 (100%)	0.35
cMRI tissular analysis*						0.33
- definite	16/35 (46%)	5/8 (63%)	6/9 (67%)	2/10 (20%)	3/8 (38%)	
- suggestive	10/35 (29%)	2/8 (25%)	2/9 (22%)	3/10 (30%)	3/8 (38%)	
- normal	9/35 (26%)	1/8 (13%)	1/9 (11%)	5/10 (50%)	2/8 (25%)	
Endomyocardial pathology*						0.03
- definite	3/32 (9%)	2/9 (22%)	0/8 (0%)	0/9 (0%)	1/6 (17%)	
- suggestive	21/32 (66%)	3/9 (33%)	4/8 (50%)	9/9 (100%)	5/6 (83%)	
- normal	8/32 (25%)	4/9 (44%)	4/8 (50%)	0/9 (0%)	0/6 (0%)	
Peripheral muscle pathology*						0.74
- definite	32 (80%)	8 (80%)	8 (80%)	8 (80%)	8 (80%)	
- suggestive	4 (10%)	1 (10%)	2 (20%)	0 (0%)	1 (10%)	
- non-specific lesions	2 (5%)	0 (0%)	0 (0%)	1 (10%)	1 (10%)	
- normal	2 (5%)	1 (10%)	0 (0%)	1 (10%)	0 (0%)	

Abbreviations: cMRI: cardiac magnetic resonance imaging

Statistics: p-values are those calculated for the comparison between quartiles, using Kruskal-Wallis and $\chi 2$-tests for trend when applied to quantitative and qualitative variables, respectively.

* See **Supplementary-Table-1** for the detailed features used for this assessment

Table 2. Severity criteria of patients included by time period of inclusion

Dates of inclusion in the consecutive quartiles (months/years)	**Overall** 05/18 - 08/21	**Quartile 1** 05/18 - 03/20	**Quartile 2** 03/20 - 12/20	**Quartile 3** 12/20 - 04/21	**Quartile 4** 05/21-08/21	**p-value**
	n/N (%), or median [interquartile range as appropriate]					
Severity Grade (at presentation)*						
Cardiac dysfunction						0.65
- Grade ≤2	39/40 (98%)	10/10(100%)	9/10 (90%)	10/10 (100%)	10/10 (100%)	
- Grade ≥3 (severe)	1/40 (2%)	0/10 (0%)	1/10 (10%)	0/10 (0%)	0/10 (0%)	
Cardiac Arrhythmia						0.16
- Grade ≤2	36/40 (90%)	8/10 (80%)	9/10 (90%)	9/10 (90%)	10/10 (100%)	
- Grade ≥3 (severe)	4/40 (10%)	2/10 (20%)	1/10 (10%)	1/10 (10%)	0/10 (0%)	
Respiratory muscle dysfunction						1
- Grade ≤2	36/40 (90%)	9/10 (90%)	9/10 (90%)	9/10 (90%)	9/10 (90%)	
- Grade ≥3 (severe)	4/40 (10%)	1/10 (10%)	1/10 (10%)	1/10 (10%)	1/10 (10%)	
Severity maximal grade*						
Cardiac dysfunction						0.06
- Grade ≤2	31/40 (78%)	5/10 (50%)	8/10 (80%)	10/0 (100%)	8/10 (80%)	
- Grade ≥3 (severe)	9/40 (22%)	5/10 (50%)	2/10 (20%)	0/10 (0%)	2/10 (20%)	
Cardiac Arrhythmias						0.26
- Grade ≤2	23/40 (58%)	4/10 (40%)	5/10 (50%)	7/10 (70%)	7/10 (70%)	
- Grade ≥3 (severe)	18/40 (45%)	6/10 (60%)	5/10 (50%)	3/10 (30%)	4/10 (40%)	
Respiratory muscle dysfunction						0.84
- Grade ≤2	23/38 (61%)	3/8 (38%)	6/10 (60%)	9/10 (90%)	5/10 (50%)	
- Grade ≥3 (severe)	15/38 (39%)	5/8 (63%)	4/10 (40%)	1/10 (10%)	5/10 (50%)	
Myotoxicity (overall)						0.74
- Grade ≤2	10/40 (25%)	2/10 (20%)	2/10 (20%)	4/10 (40%)	2/10 (20%)	
- Grade ≥3 (severe)	30/40 (75%)	8/10 (80%)	8/10 (80%)	6/10 (60%)	8/10 (80%)	
Other criteria						
Respiratory muscle involvement**						0.23
- definite	20/38 (53%)	4/8 (50%)	5/10 (50%)	8/10 (80%)	3/10 (30%)	
- probable	7/38 (18%)	2/8 (25%)	1/10 (10%)	0/10 (0%)	4/10 (40%)	
- absent	11/38 (29%)	2/8 (25%)	4/10 (40%)	2/10 (20%)	3/10 (30%)	
Type of ICI, anti-PD(L)1 (%)						0.10
- monotherapy	30 (75%)	9 (90%)	8 (80%)	7 (70%)	6 (60%)	
- combination with anti-CTLA4	10 (25%)	1 (10%)	2 (20%)	3 (30%)	4 (40%)	
Troponin-T peak value (ratio vs. 99th upper reference limit)	111 [31-175]	245 [50-991]	96 [34-157]	64 [18-153]	115 [43-150]	0.18

* See **Supplementary-Table-4 & 5** for the detailed features used for this assessment

** See **Supplementary-Table-3** for the detailed features used for this assessment

Statistics: p-values are those calculated for the comparison between quartiles, using Kruskal-Wallis and $\chi 2$-tests for trend when applied to quantitative and qualitative variables, respectively.

Figure legends.

Figure 1. Flow-Chart and evolution of the mortality in our prospective cohort of patients admitted for suspicion of ICI-myocarditis in Pitié-Salpêtrière Hospital, Paris, France

Figure 2. Troponin-T circulating levels as a function of ICI-myotoxicity severity. Evolution of circulating Troponin-T levels (cTnT, ng/L) as a surrogate for myotoxicity severity grade in the 40 ICI-myocarditis patients included in our study. All patients had increased Troponin-T levels on admission. Peak values of Troponin-T levels per patient are represented by * and track the severity grading of these patients. Five patients had grade 1 asymptomatic myocarditis, 4 of whom were not treated by any immunossupressant (but ICI withhold) and evolved favorably.

Figure 3. Examples of cardiac and skeletal muscle pathology findings on autopsies of 2 patients. Panels A-E are from a patient dead acutely from a fulminant ICI-myocarditis. Inflammatory infiltrates surrounding cardiomyocyte necrosis (A, black arrow, hematoxylin and eosin). These inflammatory infiltrates are composed by $CD3^+$ T-cells (B) and $CD68^+$ macrophages (C). Skeletal muscles were also affected by endomysial lympho-histiocytic inflammatory infiltrates and myocyte necrosis (white arrows) affecting the diaphragm (D, hematoxylin and eosin) and the psoas muscles (E, hematoxylin and eosin). Panel F is from a patient dead from COVID-19 approximatively one-year after an ICI-myocarditis episode complicated by appearance of an irreversible high-grade sinus node dysfunction requiring pacemaker implementation. Heart pathology (F, hematoxylin and eosin) revealed a complete sinus node destruction replaced by a yellowish fibrous tissue surrounding the sinoatrial nodal artery (visible within the small black square) instead of cardiomyocytes normally present. The sinus node spot is located between the superior vena cava (arrow) and the pericardium (arrowhead).

Figure 4. Effects of plasmapheresis on ICI circulating levels and immune checkpoint expression on peripheral blood mononuclear cells. While ICI concentrations were decreased by plasmapheresis, there was a surge few days after each plasmapheresis with ICI blood levels staying well above the limit of detection for months

(<1µg/mL for nivolumab; <2µg/mL for durvalumab); i.e. well above their expected IC50 (half maximal inhibitory concentration) for their PD(L)1 targets (~0.3 µg/mL for nivolumab and ~0.02µg/mL for durvalumab).(1) This phenomenon may explain why PD1 and PDL1 receptors on T-cells ($CD3^+$) and B-cells ($CD19^+$) are blocked by ICI for months after plasmapheresis. *BID: bis in die; MMF: mycophenolate mofetil*

Figure 5. **Example of the first severe ICI-myocarditis case treated with abatacept guided by real-time immune-monitoring assessment of CD86RO (CD86 receptor occupancy) on circulating monocytes.** (A) A 53yo renal cancer woman (patient #11, quartile 2, 63kilos) developed a severe ICI-myocarditis (life-threatening ventricular tachycardia, VT) 40 days after ICI start (2 doses of nivolumab & ipilimumab). CD86RO reached ~65% after 1^{st} abatacept dose with cessation of VT present at admission. After the 1^{st} plasmapheresis, abatacept level decreased in plasma from 188 to 68µg/mL. Few hours after the end of this 1^{st} pheresis, a new episode of VT recurred (CD86RO<0% at that time). Reinjection of a 2^{nd} abatacept dose was again active on stopping VT and restored CD86RO>50%. The 2^{nd} session of pheresis (drop from 203 to 72µg/mL of abatacept, before/after pheresis, respectively) was directly followed by reinjection of abatacept without any particular event. This case (#11) was the first in our cohort after instauration of a real-time CD86RO immune-monitoring assessment. Abatacept was cleared by pheresis and VT recurred. Subsequently, we stopped performing plasmapheresis (initially thought to eliminate ICI) while treating severe ICI-myocarditis cases with abatacept. Indeed, we also identified that plasmapheresis was inefficient to acutely restore PD1 and PDL1 expression on T-cells despite clearing significant amount of ICI from plasma (**Figure 4**). (B) Gating strategy for CD86 expression analysis in monocytes and CD86RO calculation. Circulating monocytes were gated in leukocytes as $CD45^+CD14^+$ cells. CD86 mean fluorescence intensity (MFI) by monocytes was then analyzed and compared to an isotypic control. Panel B shows a representative labeling at baseline before abatacept treatment and at a time-point within 72hours after injection.(21) The formula used to calculate CD86RO is exemplified in practice in this latter panel.

Figure 6. **Abatacept binds its target CD86 on circulating monocytes dose-dependently.** (A) Evolution of CD86 receptor occupancy (CD86RO) on circulating monocytes after abatacept injections as a function of the various

dose injected in the severe patients treated by abatacept in Q2-4 (n=22). Data after the 7th injection are not shown (n=2 patients). (B) Correlation (spearman) between delta CD86RO (maximal value within 72h after each abatacept injection compared to the baseline just before each injection) and doses of abatacept injected.

Figure 7. **Overall survival and cancer related outcomes in our cohort.** Overall survival since ICI start (A) or ICI-myocarditis presentation (B). Cancer progression free survival since ICI start (C) or ICI-myocarditis presentation (D) in patients surviving ICI-myotoxicity. Best change from baseline in tumor burden in patients surviving myotoxicity as a function of their cancer type (E) and immunosuppressants already received (F). For the latter analysis, 4 patients receiving ICI in adjuvant setting were excluded and one patient died before its evaluation. Among the 28 remaining patients, eight (8/28, 29%) had partial response, fifteen (15/28, 54%) had stable disease and five (5/28, 18%) had progressive disease using RECIST 1.1 criteria.(48)

Figure 8. **JAK-STAT pathway, particularly JAK2 (i.e ruxolitinib target) is upregulated in ICI-myocarditis mice and patients.** (A) Heatmap of differentially regulated genes in ICI-myocarditis (*Ctla4*$^{+/-}$ Pd1$^{-/-}$ mice, n=3) in comparison with unaffected control (*Ctla4*$^{+/+}$ Pd1$^{-/-}$ mice, n=4). (B) Gene expression of JAK and STAT family in ICI-myocarditis (*Ctla4*$^{+/-}$ Pd1$^{-/-}$ mice, n=3) in comparison with unaffected control (*Ctla4*$^{+/+}$; Pd1$^{-/-}$ mice, n=4). (C) Expression of the genes in each JAK-STAT signaling pathway in ICI-myocarditis (*Ctla4*$^{+/-}$ Pd1$^{-/-}$ mice, n=3) in comparison with unaffected control (*Ctla4*$^{+/+}$; Pd1$^{-/-}$ mice, n=4). (D) Gene expression of JAK and STAT family in ICI-myocarditis patients (ICIM, *n*=9), in comparison with ICI-treated patients without myocarditis (ICI-control, *n*=4).

Figure 1.

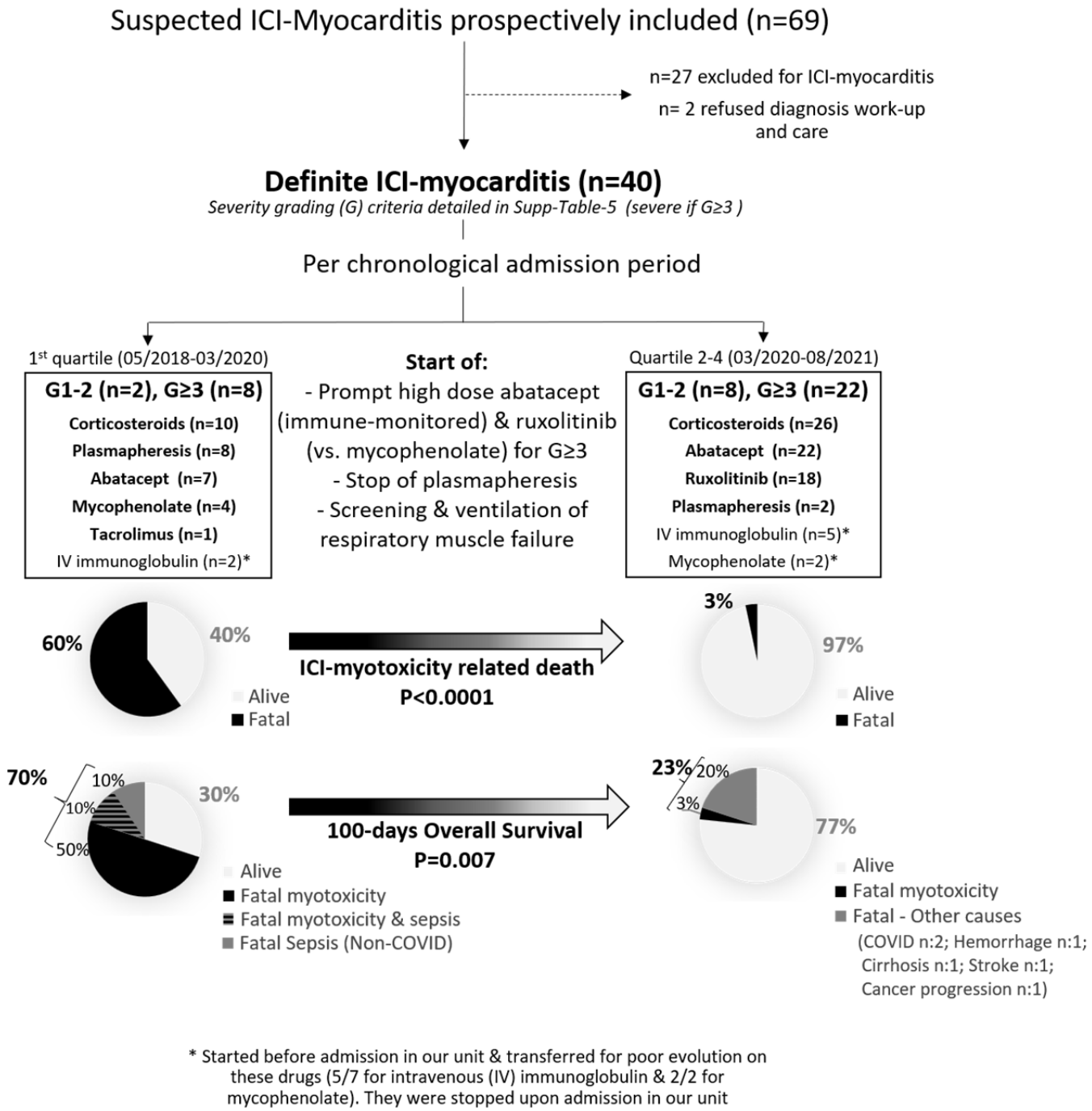

* Started before admission in our unit & transferred for poor evolution on these drugs (5/7 for intravenous (IV) immunoglobulin & 2/2 for mycophenolate). They were stopped upon admission in our unit

Figure 2.

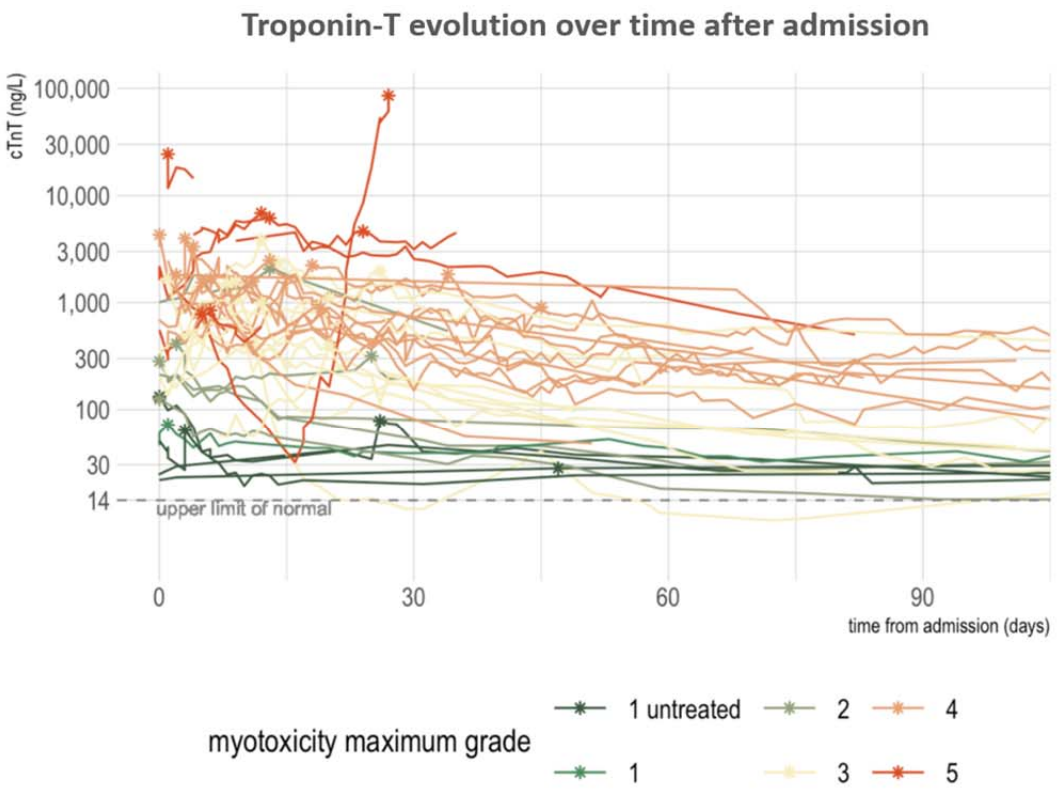

*See **Supplementary Table 5** for extended details concerning severity grading criteria.

Myotoxicity severity criteria*

Grade 1 (mild)	Asymptomatic with abnormal cardiac biomarker testing (troponin) potentially associated with mild ECG or LVEF abnormalities (no severity criteria)
Grade 2 (moderate)	Mild symptoms with abnormal cardiac biomarker testing (troponin) with moderate LVEF or ECG abnormalities
Grade 3 (Severe)	Abnormal cardiac biomarker testing (troponin) with appearance of severe cardiac pro-arrhythmias, or acute heart failure (but not cardiogenic shock) or concurrent respiratory muscle failure leading to hypoventilation (but no urgent need for mechanical ventilation) or cortico-resistance
Grade 4 (life-threatening)	**Abnormal cardiac biomarker testing (troponin) with sustained/symptomatic cardiac arrythmias or cardiogenic shock; or concurrent overt respiratory muscle failure requiring urgent mechanical ventilation.**
Grade 5 (fatal)	**Fatal**

Figure 3.

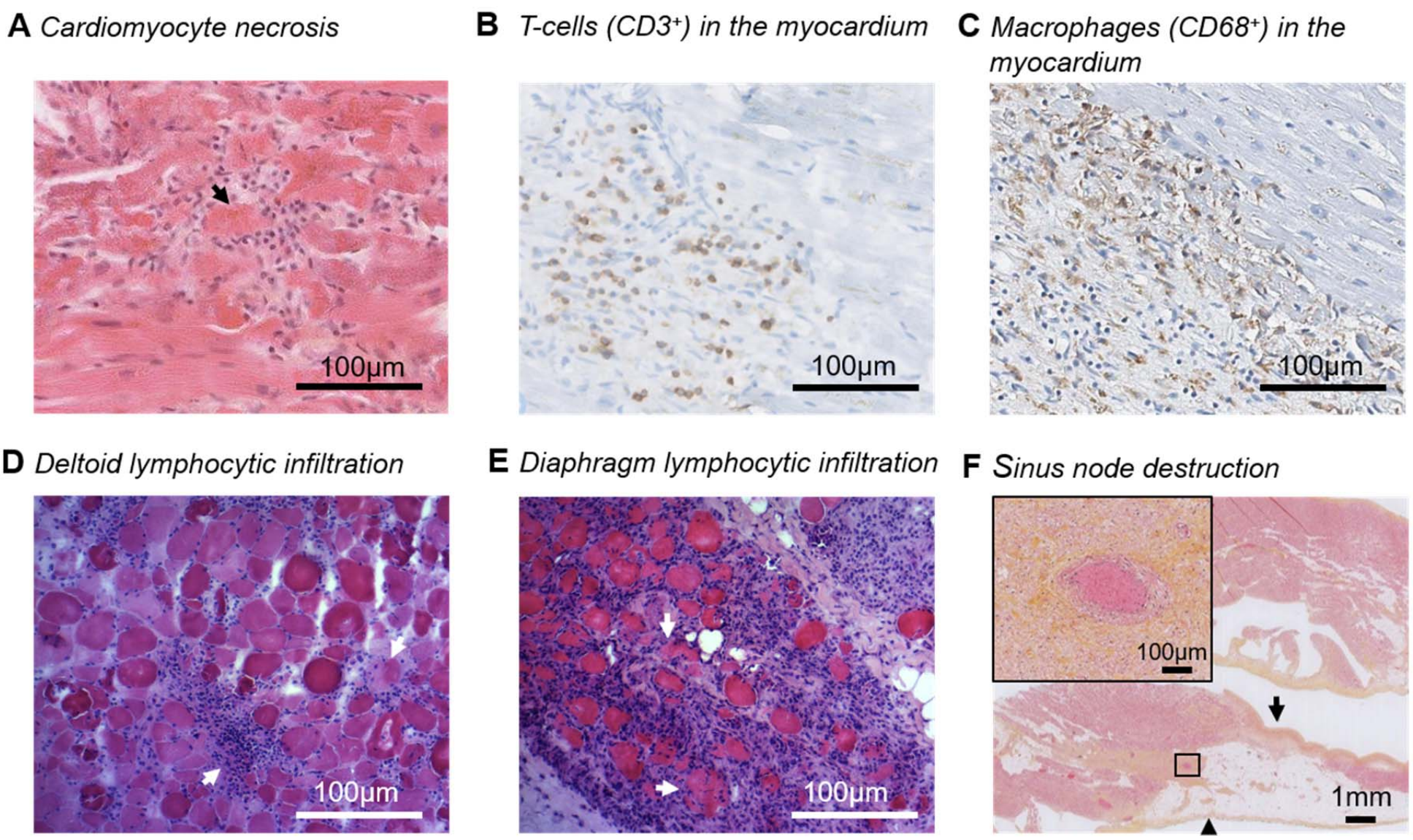
A Cardiomyocyte necrosis
100µm
B T-cells (CD3+) in the myocardium
100µm
C Macrophages (CD68+) in the myocardium
100µm
D Deltoid lymphocytic infiltration
100µm
E Diaphragm lymphocytic infiltration
100µm
F Sinus node destruction
100µm
1mm

Figure 4.

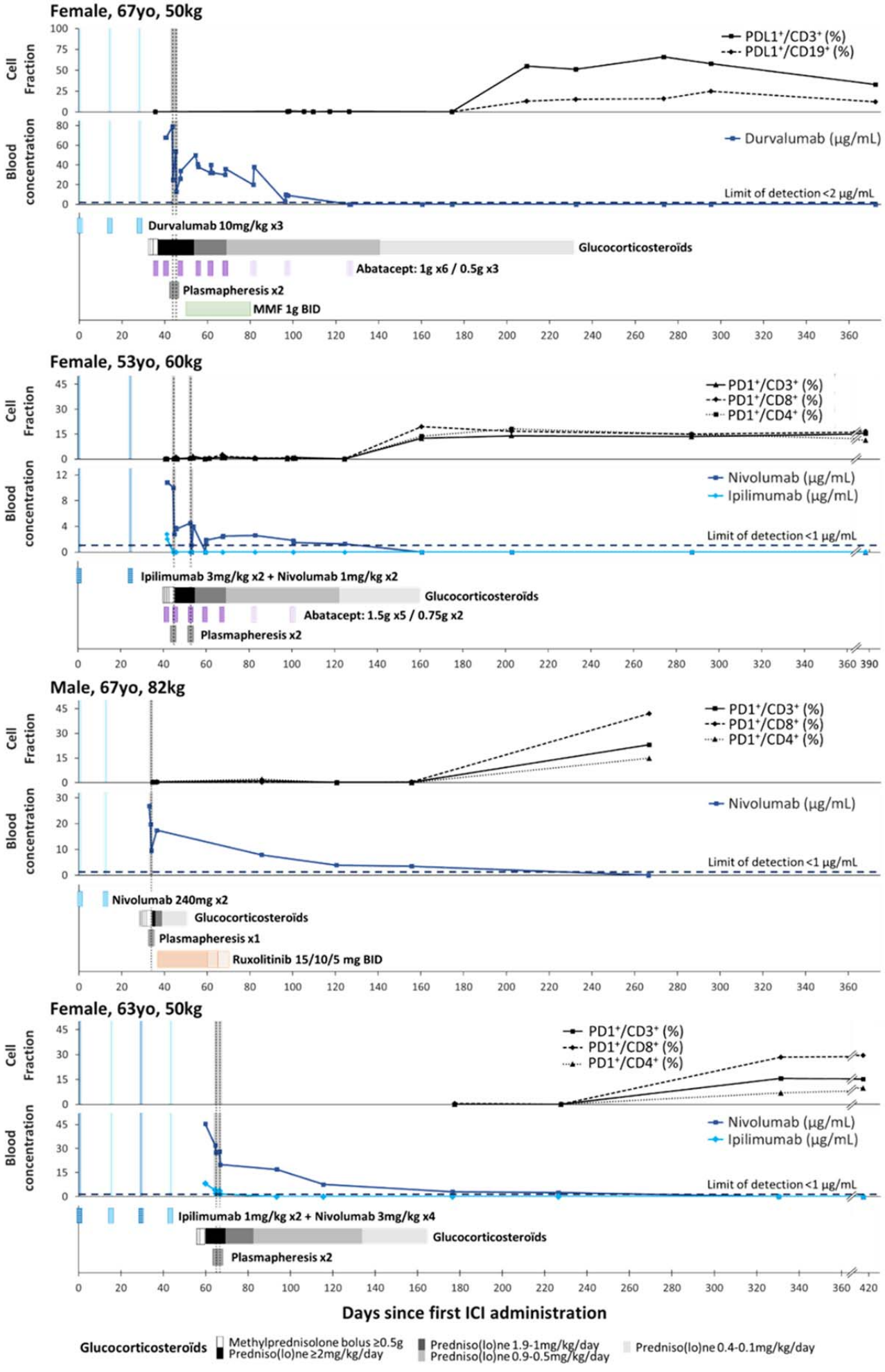
Female, 67yo, 50kg
Cell Fraction
PDL1+/CD3+ (%)
PDL1+/CD19+ (%)
Blood concentration
Durvalumab (µg/mL)
Limit of detection <2 µg/mL
Durvalumab 10mg/kg x3
Glucocorticosteroïds
Abatacept: 1g x6 / 0.5g x3
Plasmapheresis x2
MMF 1g BID
Female, 53yo, 60kg
PD1+/CD3+ (%)
PD1+/CD8+ (%)
PD1+/CD4+ (%)
Nivolumab (µg/mL)
Ipilimumab (µg/mL)
Limit of detection <1 µg/mL
Ipilimumab 3mg/kg x2 + Nivolumab 1mg/kg x2
Glucocorticosteroïds
Abatacept: 1.5g x5 / 0.75g x2
Plasmapheresis x2
Male, 67yo, 82kg
Nivolumab 240mg x2
Glucocorticosteroïds
Plasmapheresis x1
Ruxolitinib 15/10/5 mg BID
Female, 63yo, 50kg
Ipilimumab 1mg/kg x2 + Nivolumab 3mg/kg x4
Glucocorticosteroïds
Plasmapheresis x2
Days since first ICI administration
Glucocorticosteroïds
Methylprednisolone bolus ≥0.5g
Predniso(lo)ne ≥2mg/kg/day
Predniso(lo)ne 1.9-1mg/kg/day
Predniso(lo)ne 0.9-0.5mg/kg/day
Predniso(lo)ne 0.4-0.1mg/kg/day

Figure 5.

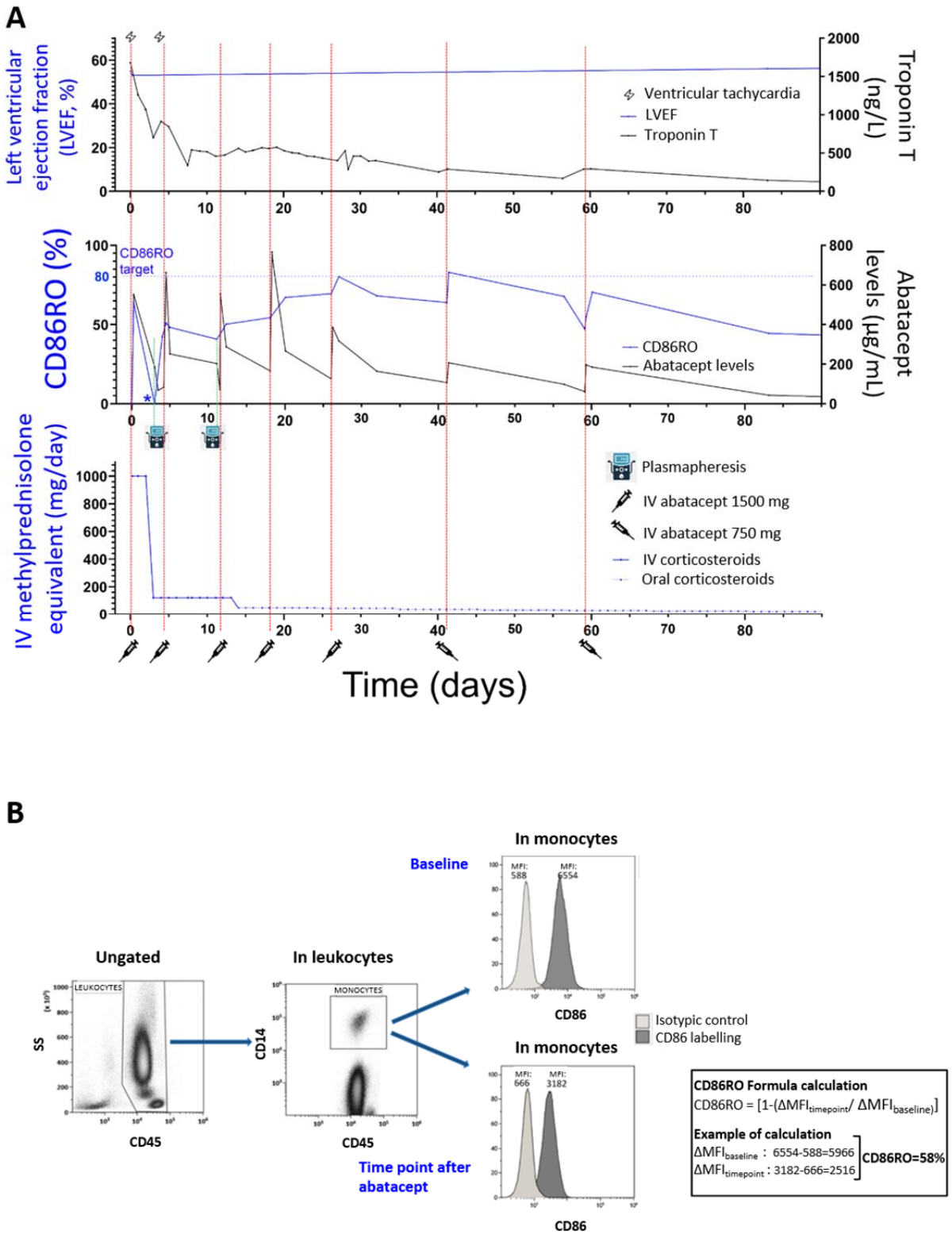

*For graphical representation, negative values of CD86RO were represented as null.

Figure 6.

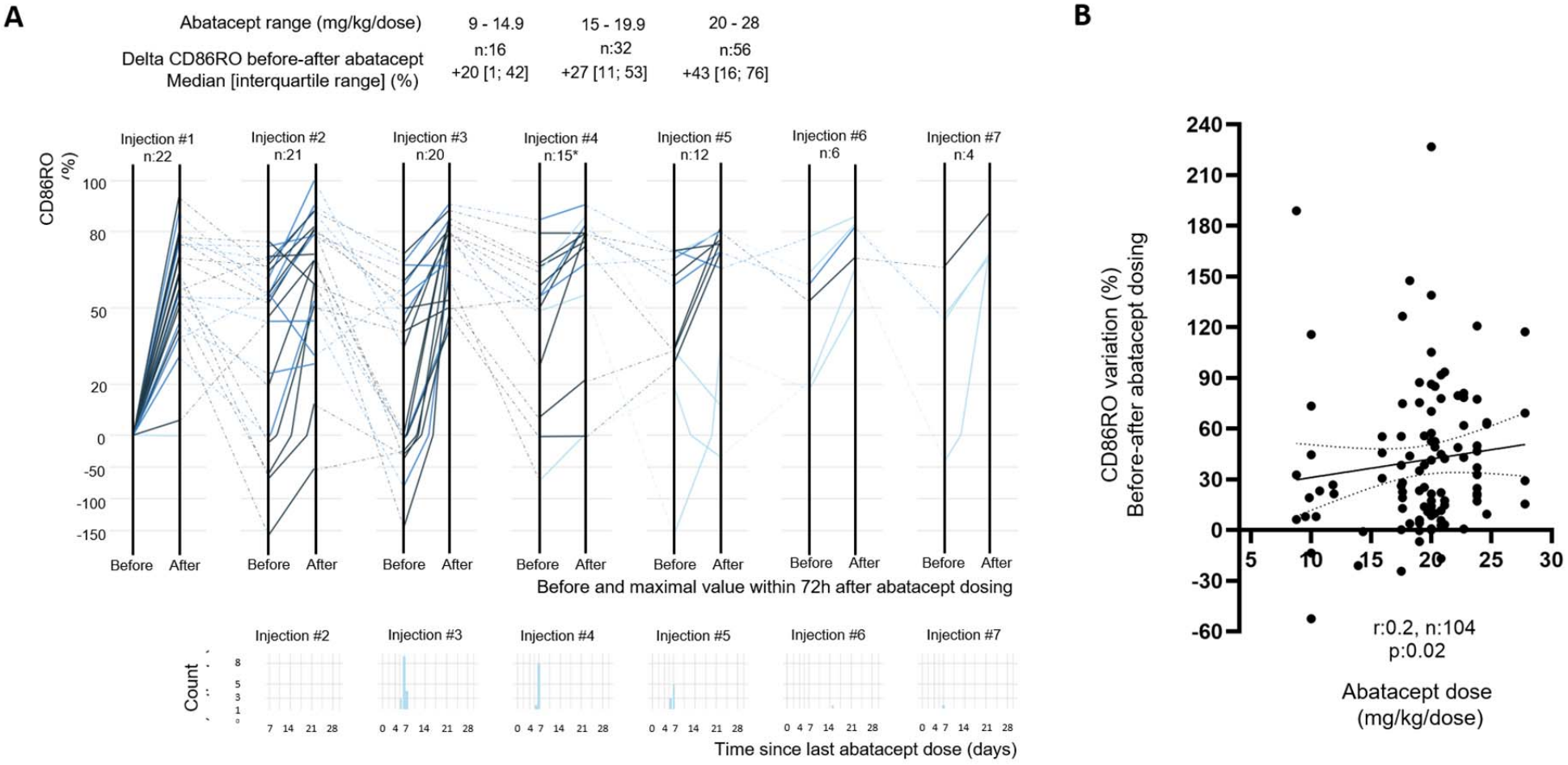

* One CD86RO value was not evaluated due to technical issues

Figure 7.

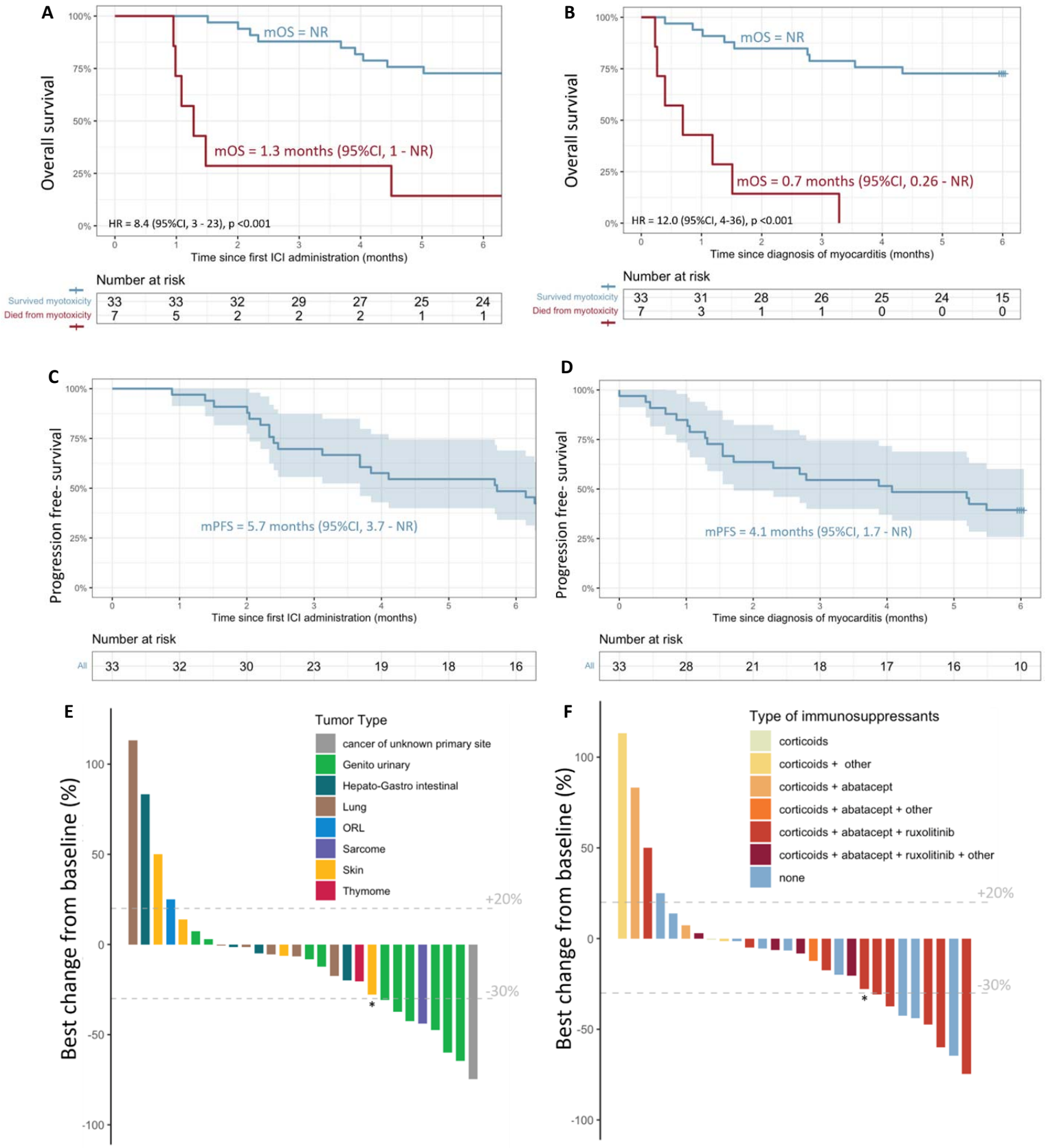

* Progressive disease due to appearance of new tumoral lesions

Abbreviations: HR, hazard ratio; ICI, immune checkpoint inhibitors; mOS, median overall survival; NR, not reached; mOS, median overall survival; mPFS, median progression free survival

Figure 8.

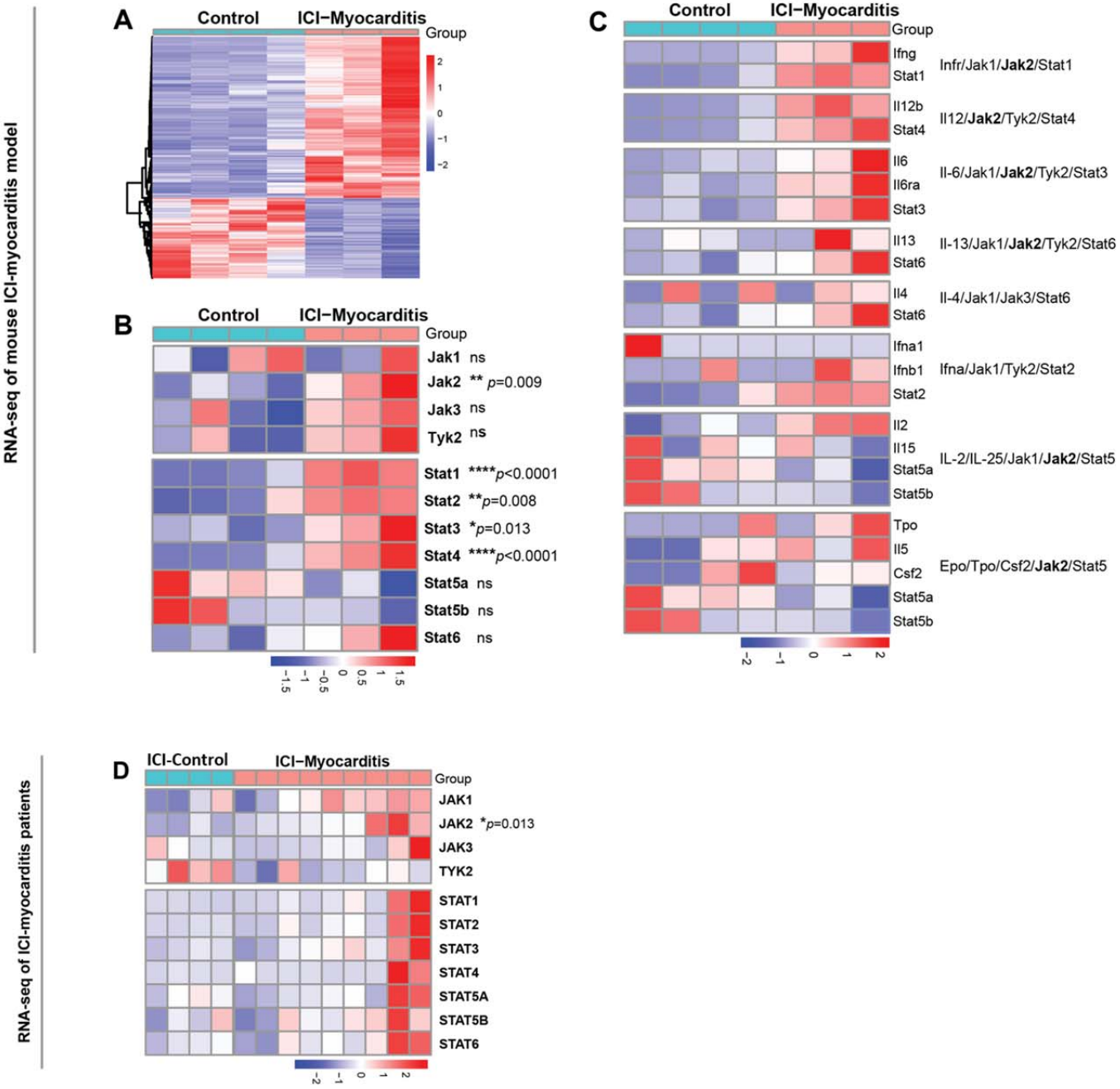
RNA-seq of mouse ICI-myocarditis model
A
Control
ICI−Myocarditis
Group
B
Control
ICI−Myocarditis
Group
Jak1 ns
Jak2 ** p=0.009
Jak3 ns
Tyk2 ns
Stat1 ****p<0.0001
Stat2 **p=0.008
Stat3 *p=0.013
Stat4 ****p<0.0001
Stat5a ns
Stat5b ns
Stat6 ns
C
Control
ICI−Myocarditis
Group
Ifng
Stat1
Infr/Jak1/Jak2/Stat1
Il12b
Stat4
Il12/Jak2/Tyk2/Stat4
Il6
Il6ra
Stat3
Il-6/Jak1/Jak2/Tyk2/Stat3
Il13
Stat6
Il-13/Jak1/Jak2/Tyk2/Stat6
Il4
Stat6
Il-4/Jak1/Jak3/Stat6
Ifna1
Ifnb1
Stat2
Ifna/Jak1/Tyk2/Stat2
Il2
Il15
Stat5a
Stat5b
IL-2/IL-25/Jak1/Jak2/Stat5
Tpo
Il5
Csf2
Stat5a
Stat5b
Epo/Tpo/Csf2/Jak2/Stat5
RNA-seq of ICI-myocarditis patients
D
ICI-Control
ICI−Myocarditis
Group
JAK1
JAK2 *p=0.013
JAK3
TYK2
STAT1
STAT2
STAT3
STAT4
STAT5A
STAT5B
STAT6

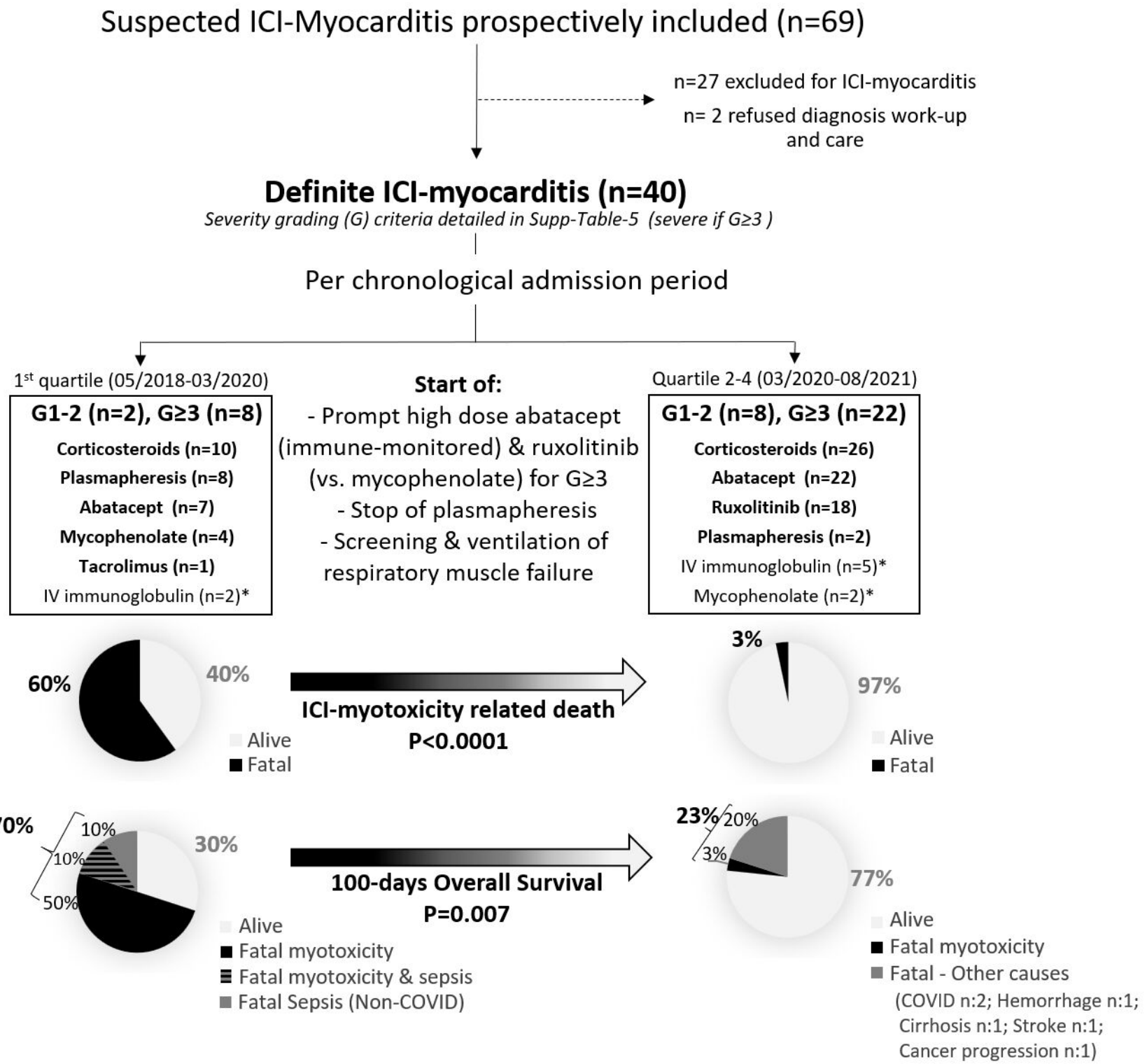

* Started before admission in our unit & transferred for poor evolution on these drugs (5/7 for intravenous (IV) immunoglobulin & 2/2 for mycophenolate). They were stopped upon admission in our unit

Troponin-T evolution over time after admission

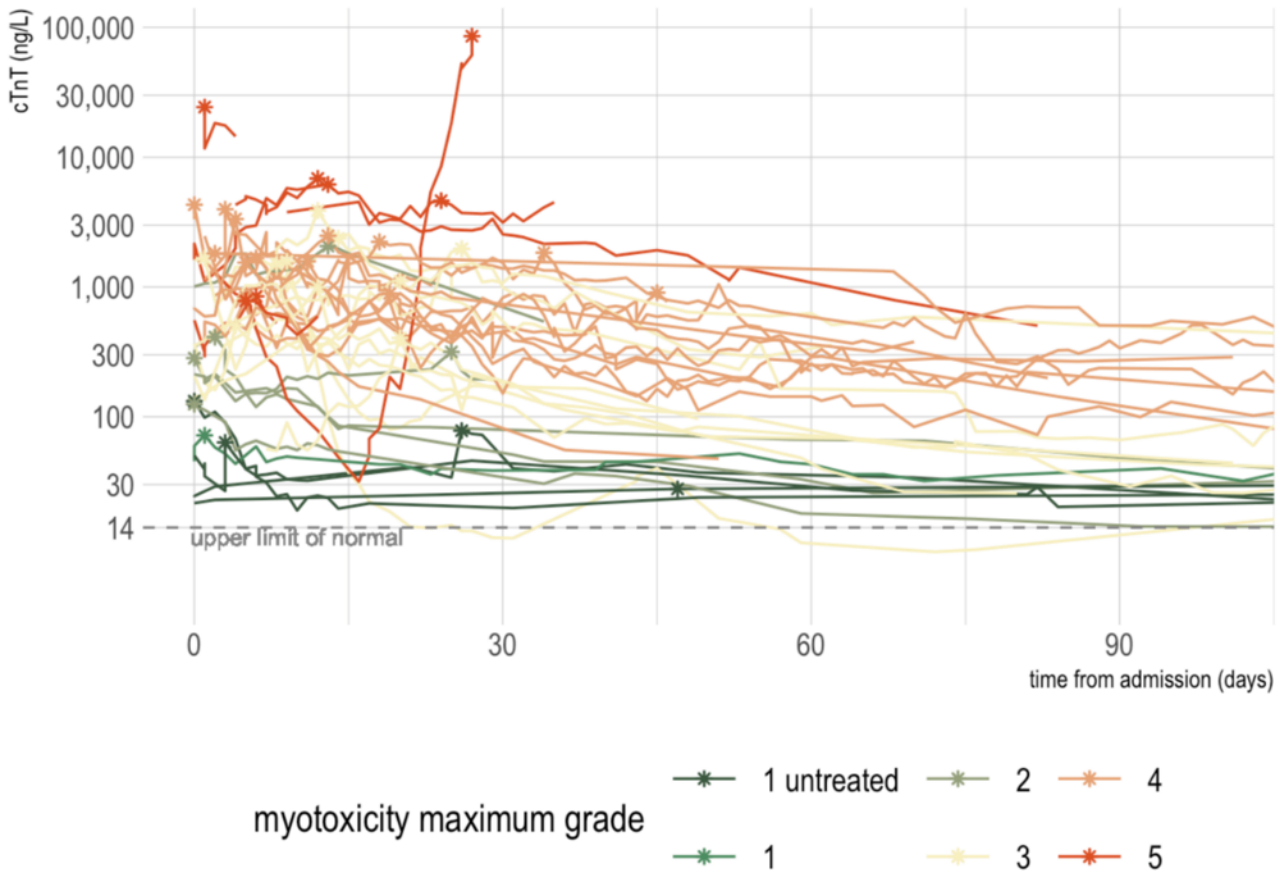

*See **Supplementary Table 5** for extended details concerning severity grading criteria.

Myotoxicity severity criteria*

Grade 1 (mild)	Asymptomatic with abnormal cardiac biomarker testing (troponin) potentially associated with mild ECG or LVEF abnormalities (no severity criteria)
Grade 2 (moderate)	Mild symptoms with abnormal cardiac biomarker testing (troponin) with moderate LVEF or ECG abnormalities
Grade 3 (Severe)	Abnormal cardiac biomarker testing (troponin) with appearance of severe cardiac pro-arrhythmias, or acute heart failure (but not cardiogenic shock) or concurrent respiratory muscle failure leading to hypoventilation (but no urgent need for mechanical ventilation) or cortico-resistance
Grade 4 (life-threatening)	**Abnormal cardiac biomarker testing (troponin) with sustained/symptomatic cardiac arrythmias or cardiogenic shock; or concurrent overt respiratory muscle failure requiring urgent mechanical ventilation.**
Grade 5 (fatal)	**Fatal**

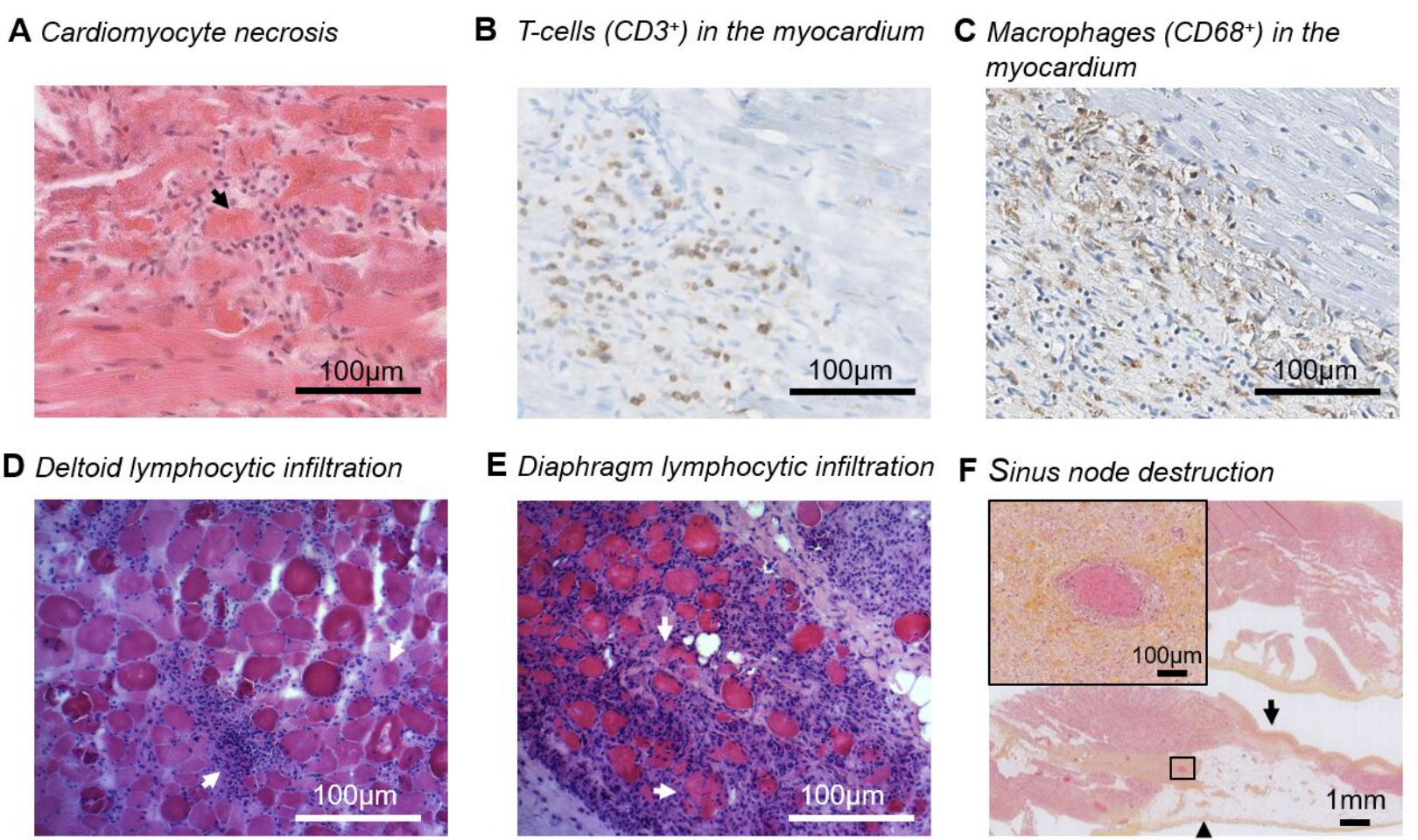
A Cardiomyocyte necrosis
100µm
B T-cells (CD3+) in the myocardium
100µm
C Macrophages (CD68+) in the myocardium
100µm
D Deltoid lymphocytic infiltration
100µm
E Diaphragm lymphocytic infiltration
100µm
F Sinus node destruction
100µm
1mm

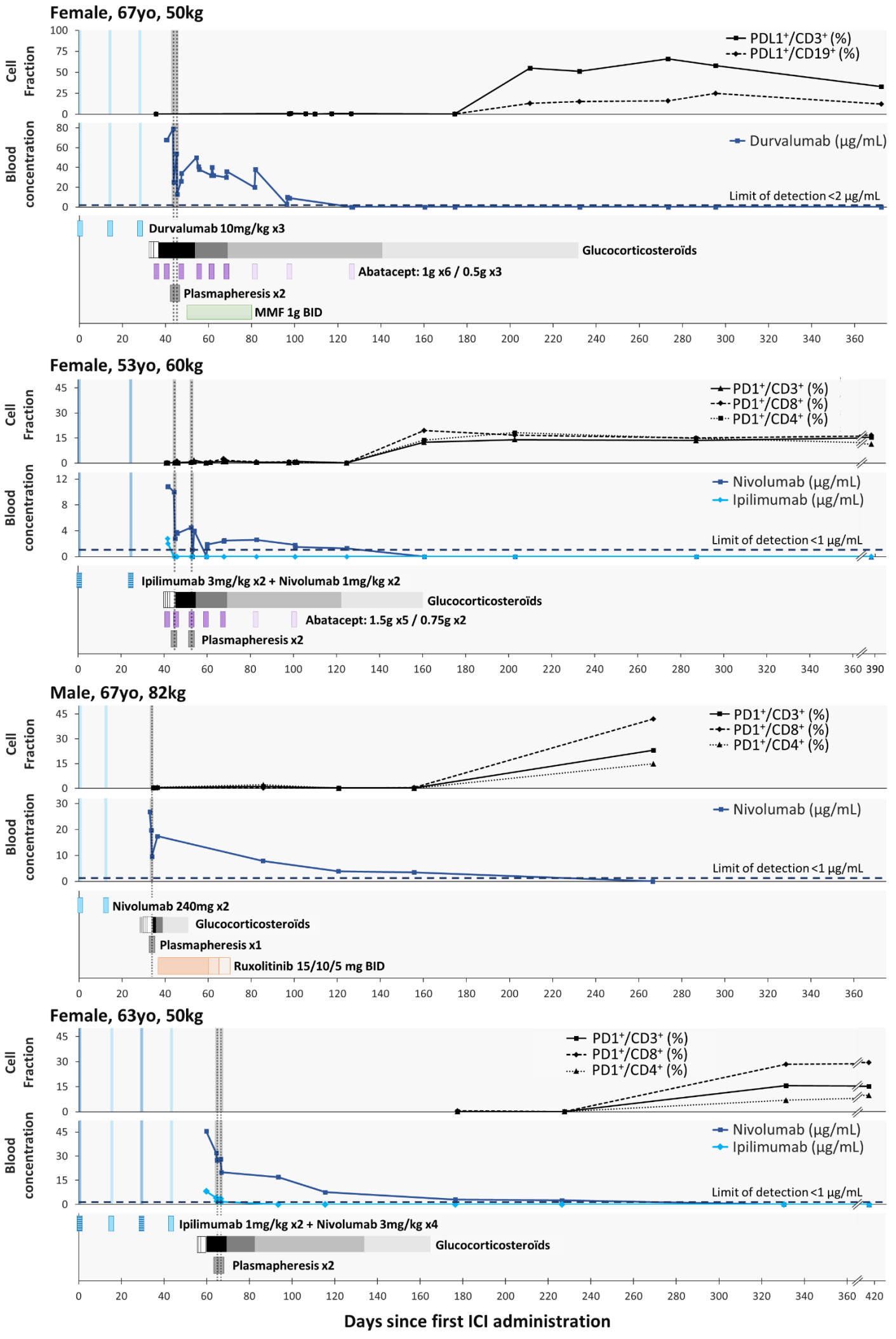
Female, 67yo, 50kg
Cell Fraction
PDL1+/CD3+ (%)
PDL1+/CD19+ (%)
Blood concentration
Durvalumab (µg/mL)
Limit of detection <2 µg/mL
Durvalumab 10mg/kg x3
Glucocorticosteroïds
Abatacept: 1g x6 / 0.5g x3
Plasmapheresis x2
MMF 1g BID
Female, 53yo, 60kg
PD1+/CD3+ (%)
PD1+/CD8+ (%)
PD1+/CD4+ (%)
Nivolumab (µg/mL)
Ipilimumab (µg/mL)
Limit of detection <1 µg/mL
Ipilimumab 3mg/kg x2 + Nivolumab 1mg/kg x2
Glucocorticosteroïds
Abatacept: 1.5g x5 / 0.75g x2
Plasmapheresis x2
Male, 67yo, 82kg
PD1+/CD3+ (%)
PD1+/CD8+ (%)
PD1+/CD4+ (%)
Nivolumab (µg/mL)
Limit of detection <1 µg/mL
Nivolumab 240mg x2
Glucocorticosteroïds
Plasmapheresis x1
Ruxolitinib 15/10/5 mg BID
Female, 63yo, 50kg
PD1+/CD3+ (%)
PD1+/CD8+ (%)
PD1+/CD4+ (%)
Nivolumab (µg/mL)
Ipilimumab (µg/mL)
Limit of detection <1 µg/mL
Ipilimumab 1mg/kg x2 + Nivolumab 3mg/kg x4
Glucocorticosteroïds
Plasmapheresis x2
Days since first ICI administration
Glucocorticosteroïds
Methylprednisolone bolus ≥0.5g
Predniso(lo)ne ≥2mg/kg/day
Predniso(lo)ne 1.9-1mg/kg/day
Predniso(lo)ne 0.9-0.5mg/kg/day
Predniso(lo)ne 0.4-0.1mg/kg/day

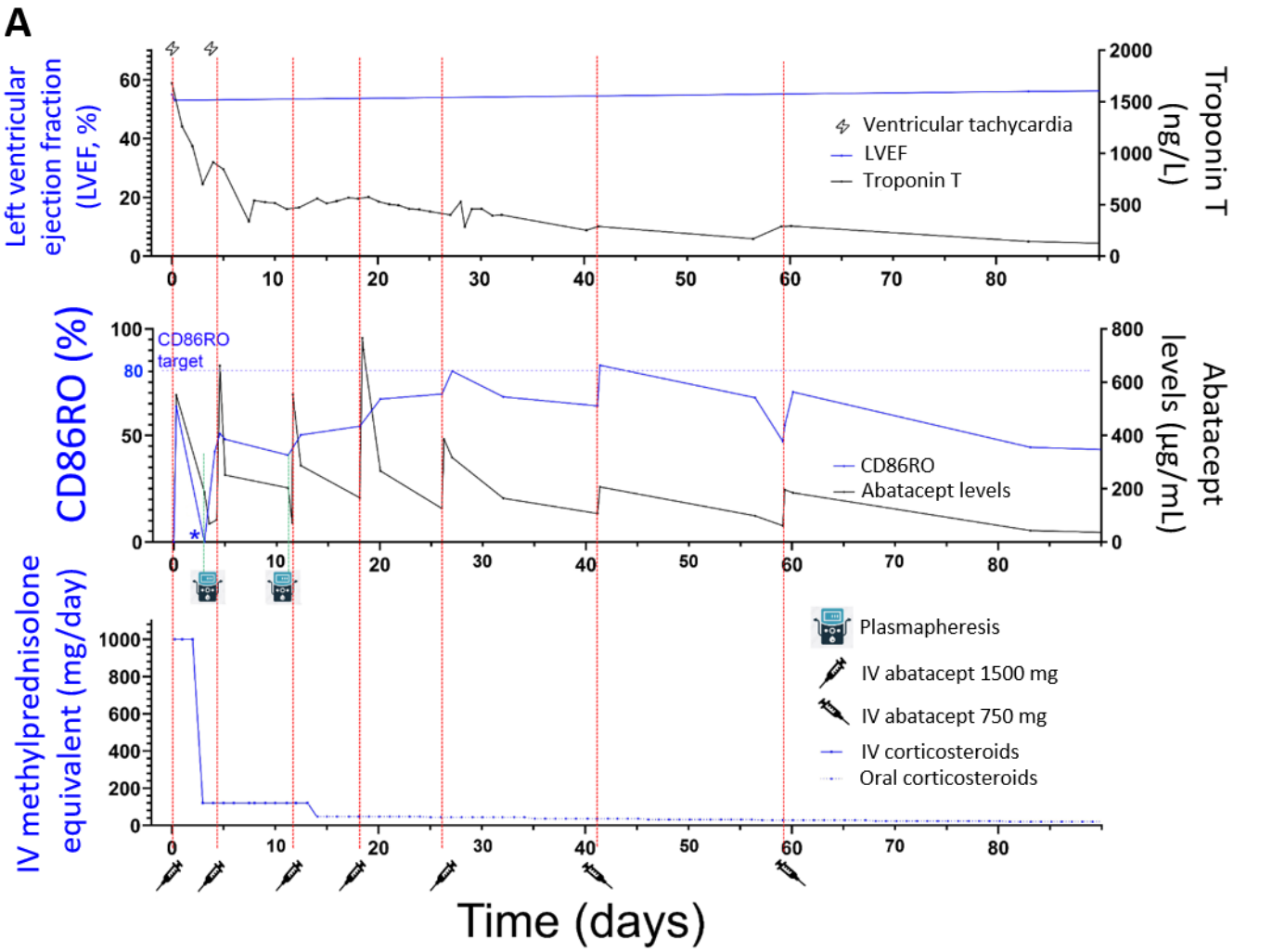
A
Left ventricular ejection fraction (LVEF, %)
Troponin T (ng/L)
Ventricular tachycardia
LVEF
Troponin T
CD86RO (%)
CD86RO target
Abatacept levels (µg/mL)
CD86RO
Abatacept levels
IV methylprednisolone equivalent (mg/day)
Plasmapheresis
IV abatacept 1500 mg
IV abatacept 750 mg
IV corticosteroids
Oral corticosteroids
Time (days)

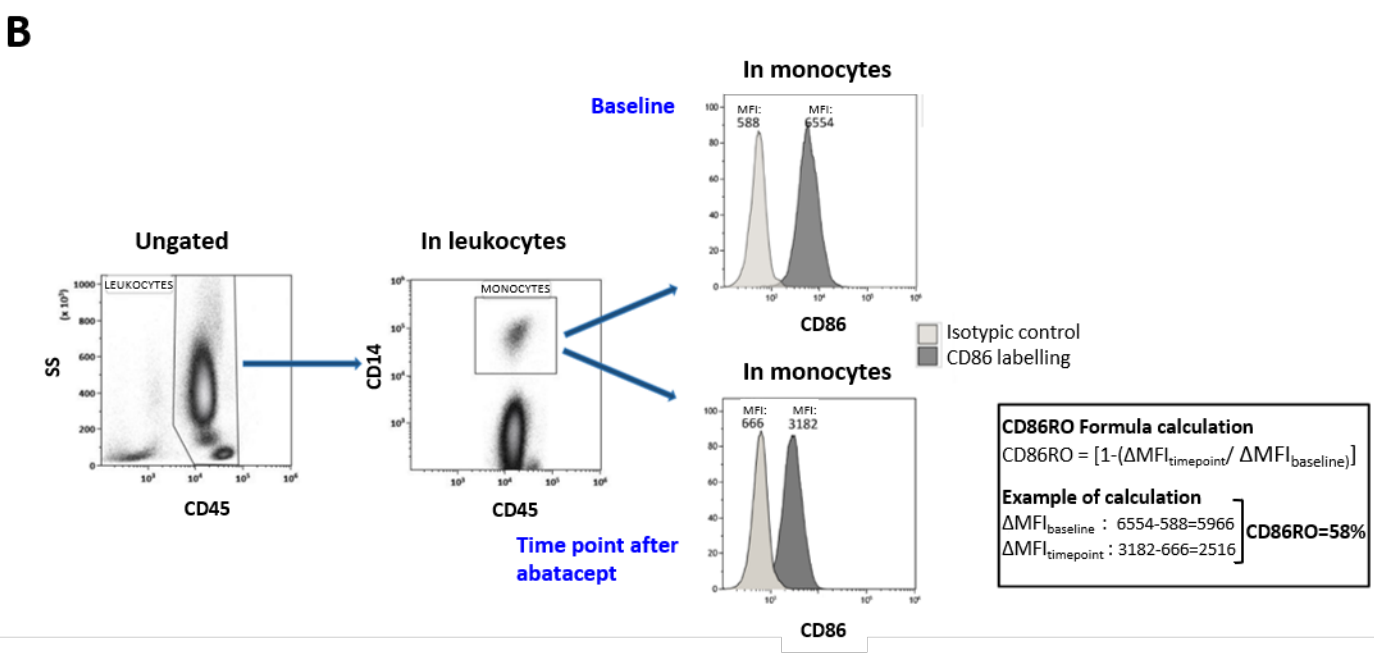
B
Ungated
In leukocytes
In monocytes
Baseline
LEUKOCYTES
MONOCYTES
SS
CD14
CD45
CD86
MFI: 588
MFI: 6554
MFI: 666
MFI: 3182
Isotypic control
CD86 labelling
Time point after abatacept
CD86RO Formula calculation
CD86RO = [1-(ΔMFI timepoint/ ΔMFI baseline)]
Example of calculation
ΔMFI baseline : 6554-588=5966
ΔMFI timepoint : 3182-666=2516
CD86RO=58%

A

Abatacept range (mg/kg/dose)	9 - 14.9	15 - 19.9	20 - 28
Delta CD86RO before-after abatacept Median [interquartile range] (%)	n:16 +20 [1; 42]	n:32 +27 [11; 53]	n:56 +43 [16; 76]

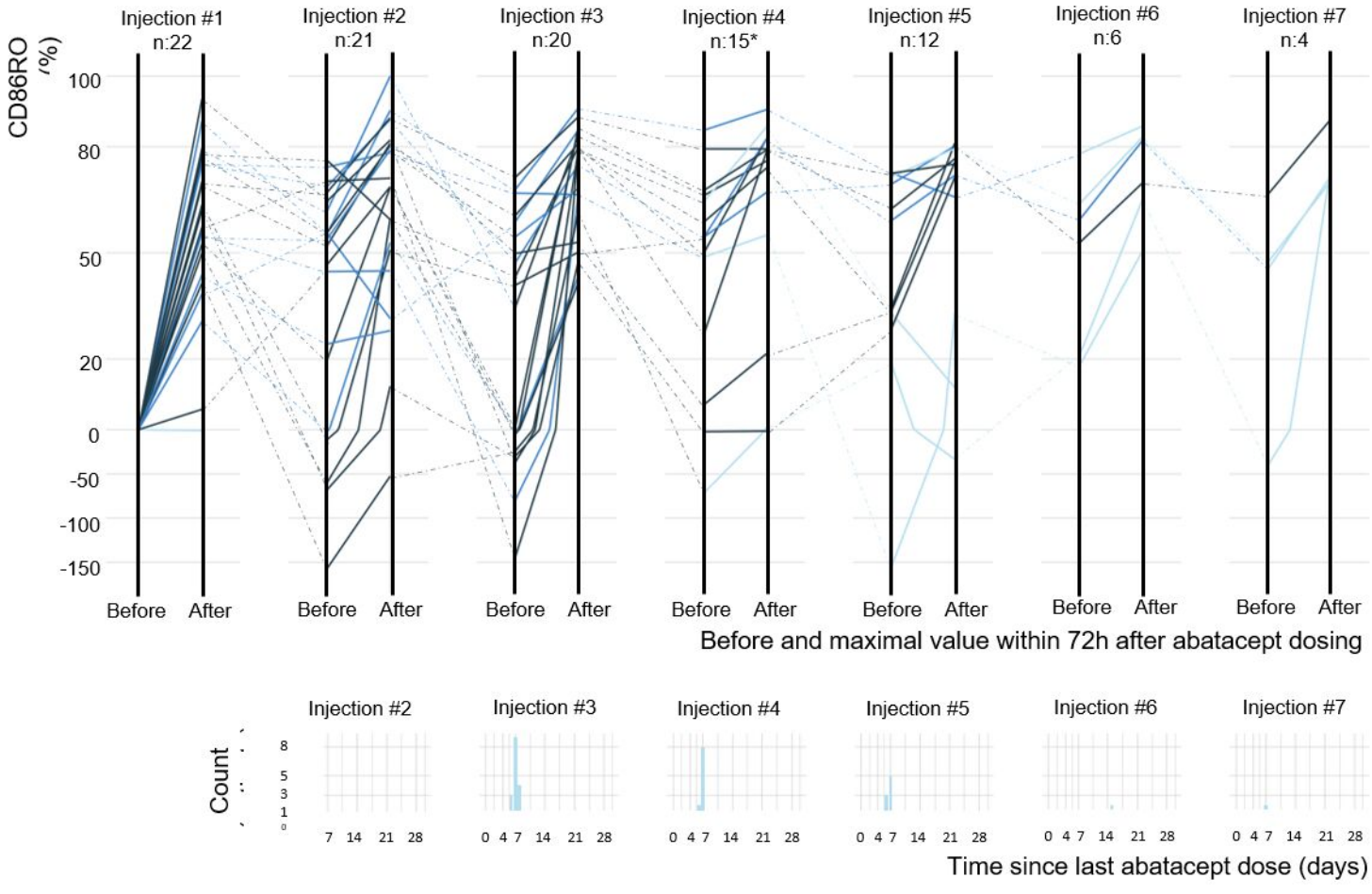

* One CD86RO value was not evaluated due to technical issues

B

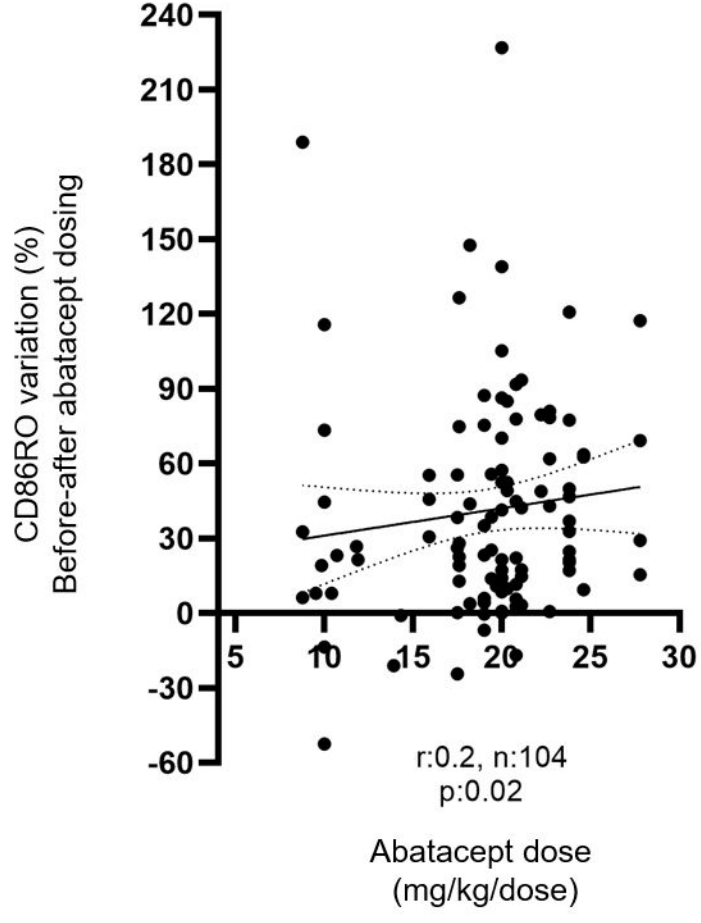

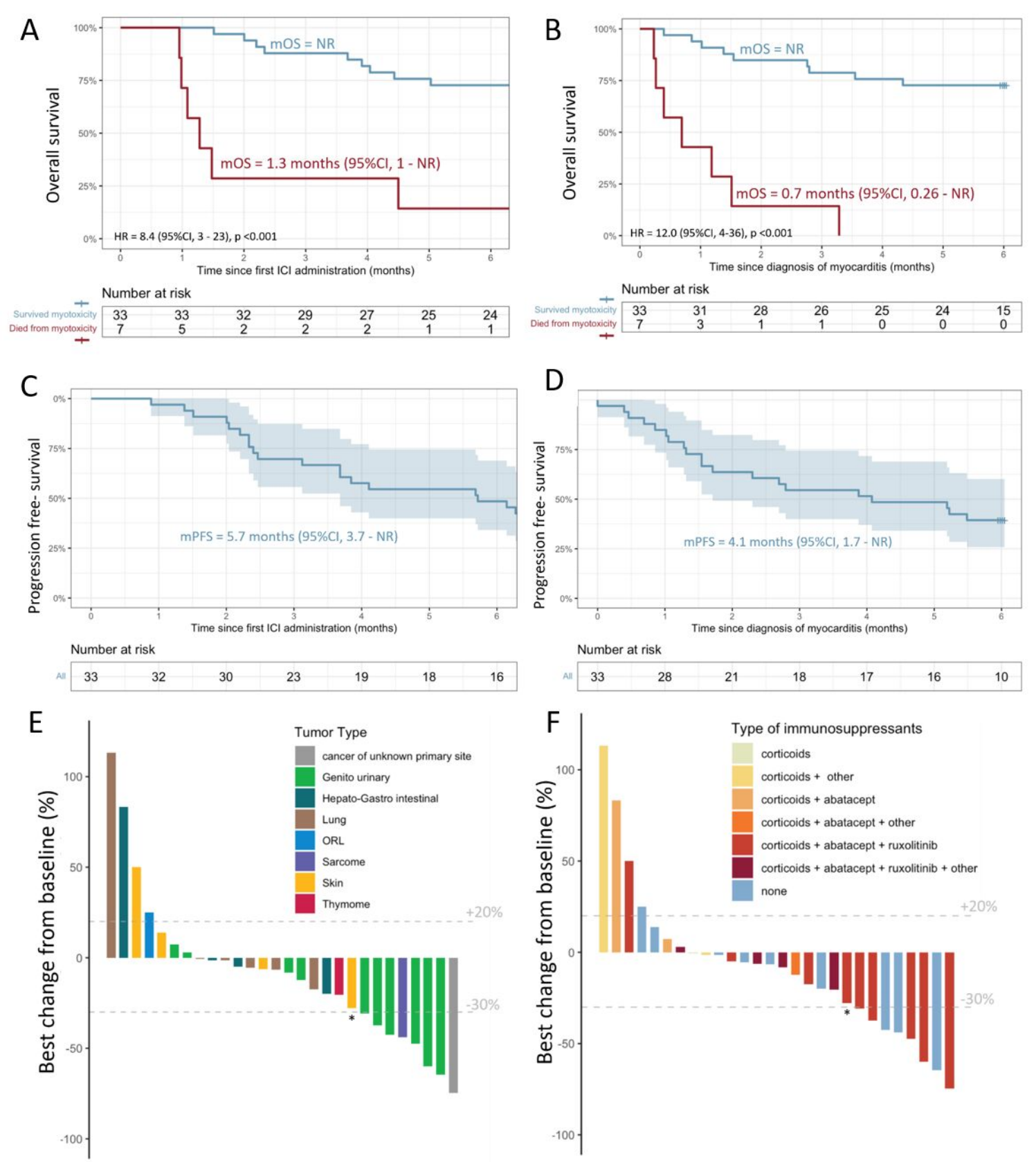

* Progressive disease due to appearance of new tumoral lesions

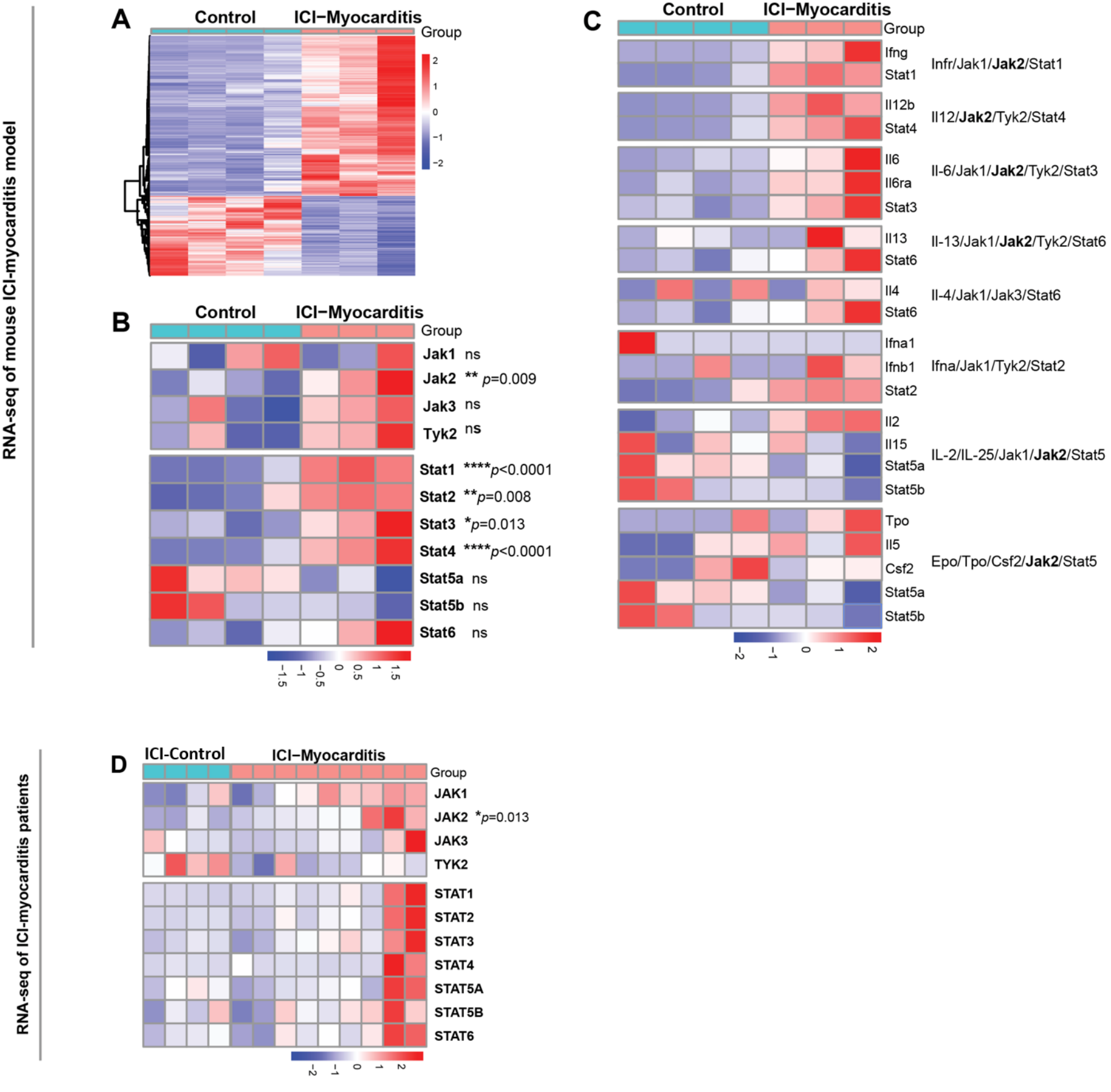
RNA-seq of mouse ICI-myocarditis model
A
Control
ICI−Myocarditis
Group
2
1
0
−1
−2
B
Control
ICI−Myocarditis
Group
Jak1 ns
Jak2 ** p=0.009
Jak3 ns
Tyk2 ns
Stat1 ****p<0.0001
Stat2 **p=0.008
Stat3 *p=0.013
Stat4 ****p<0.0001
Stat5a ns
Stat5b ns
Stat6 ns
−1.5
−1
−0.5
0
0.5
1
1.5
C
Control
ICI−Myocarditis
Group
Ifng
Stat1
Infr/Jak1/Jak2/Stat1
Il12b
Stat4
Il12/Jak2/Tyk2/Stat4
Il6
Il6ra
Stat3
Il-6/Jak1/Jak2/Tyk2/Stat3
Il13
Stat6
Il-13/Jak1/Jak2/Tyk2/Stat6
Il4
Stat6
Il-4/Jak1/Jak3/Stat6
Ifna1
Ifnb1
Stat2
Ifna/Jak1/Tyk2/Stat2
Il2
Il15
Stat5a
Stat5b
IL-2/IL-25/Jak1/Jak2/Stat5
Tpo
Il5
Csf2
Stat5a
Stat5b
Epo/Tpo/Csf2/Jak2/Stat5
−2
−1
0
1
2
RNA-seq of ICI-myocarditis patients
D
ICI-Control
ICI−Myocarditis
Group
JAK1
JAK2 *p=0.013
JAK3
TYK2
STAT1
STAT2
STAT3
STAT4
STAT5A
STAT5B
STAT6
−2
−1
0
1
2